RSC Advances

ROYAL SOCIETY OF CHEMISTRY

www.rsc.org/advances

NHC Macrometallocycles of Mercury(II) and Silver(I): Synthesis, Structural Studies and Recognition of Hg(II) Complex 4 for Silver ion

Qing-Xiang Liu,* Qing Wei, Rui Liu, Xiao-Jun Zhao and Zhi-Xiang Zhao
Tianjin Key Laboratory of Structure and Performance for Functional Molecules; Key Laboratory of Inorganic-Organic Hybrid Functional Material Chemistry, Ministry of Education; College of Chemistry, Tianjin Normal University, Tianjin 300387, China.
* Corresponding author, E-mail: tjnulqx@163.com

Abstract: A series of bis-benzimidazolium (or bis-imidazolium) salts, and their seven N-heterocyclic carbene mercury(II) and silver(I) complexes **2-8**, as well as one anionic complex **1** have been synthesized and characterized. In complex **1**, two benzimidazole rings point to opposite directions, and π-π interactions between these two benzimidazole rings are observed. In complex **2**, two 13-membered macrometallocycles are linked together by one bridging chlorine atom, in which each macrometallocycle is formed by one bidentate carbene ligand (**L^2**) and one Hg(II) ion. In complexes **3-6**, each molecule contains one 13-membered macrometallocycle formed via one bidentate carbene ligand and one metal ion. In the crystal packings of **1-8**, 1D polymeric chains, 2D supramolecular layers and 3D supramolecular frameworks are formed via intermolecular weak interactions, including hydrogen bonds, π-π interactions and C-H···π contacts. Particularly, the selective recognition of Ag$^+$ using **4** as a host compound was studied on the basis of fluorescent and UV/vis spectroscopic titrations.

Keywords: N-heterocyclic carbene, silver(I), mercury(II), recognition.

Introduction

The fluorescent recognition is one of significant tools to detect and measure metal ions in chemistry, biology and environmental science.[1] So far, a number of host compounds for recognition of metal ions have been reported,[2] but the development of practical host compounds is still important work for researchers. The compounds containing silver(I) ion is widely used in the electrical, photography imaging and pharmaceutical industry.[3] It is known that silver oxide can destroy the environmental benign bacteria by inhibiting their growth or disturbing their reproductive ability. Also silver(I) ion can inactivate sulfhydryl enzymes and destroy organic tissues to lead to cell death.[3(b), 4] Therefore, the detecting and monitoring content of silver(I) ion in soil, food and water have great importance for the environment and human health. There are many methods toward Ag^+ detection, such as fluorescence spectrophotometry,[5] inductively coupled plasma mass spectrometry (ICP-MS)[6] and atomic absorption spectrometry.[7] Among these methods, the fluorescence spectrophotometry has received more attention due to high sensitivity and easy-operation. In reported fluorescence host compounds for Ag^+ detection, the main binding sites are N, O, S and π system,[8] and the using I-donor of organic compound as binding site was not found although iodine has strong affinity toward Ag^+. Therefore, the design and synthesis of host compounds bearing I-donor may be a promising method for Ag^+ detection.

During the course of searching for appropriate host compounds, we become interested in N-heterocyclic carbene (NHC) metal complexes. N-heterocyclic carbene can form stable metal complexes with many transition metals due to its strong σ-donating property.[9] Among these metal complexes, NHC metal complexes based on chelating bis-NHC ligands with different linkages (such as aromatic ring and ether chain) can be used as receptors to capture selectively guests (ions or molecules),[10] and they may be a type of host compound with the value of potential application in host-guest chemistry.

In this paper, we report the preparation of bis-benzimidazolium salts 2,3-bis[2'-(N-R-benzimidazoliumyl)ethoxy]naphthalene $2X^-$ ($\mathbf{L^1H_2{\cdot}(PF_6)_2}$: R = ethyl, X = PF_6; $\mathbf{L^2H_2{\cdot}I_2}$: R = picolyl, X = I; $\mathbf{L^2H_2{\cdot}(PF_6)_2}$: R = picolyl, X = PF_6; $\mathbf{L^3H_2{\cdot}I_2}$: R = ^{n}propyl, X = I; $\mathbf{L^4H_2{\cdot}(PF_6)_2}$: R = ^{n}butyl, X = PF_6), and bis-imidazolium salts 2,3-bis[2'-(N-R-imidazoliumyl)ethoxy]naphthalene hexafluorophosphate ($\mathbf{L^5H_2{\cdot}(PF_6)_2}$: R = ^{n}butyl; $\mathbf{L^6H_2{\cdot}(PF_6)_2}$: R = ethyl), as well as preparation and structures of one anionic complex $[L^1H_2](Pd_2Cl_6)$ (**1**) and seven N-heterocyclic carbene metal complexes, $[(L^2HgI)_2Cl]I$ (**2**), $[L^3Hg(HgCl_2I_2)]$ (**3**), $[L^4HgI_2]$ (**4**),

[L^5HgI_2] (**5**), [$L^6Hg(HgI_4)(DMSO)$] (**6**), [L^2Ag](PF_6) (**7**) and [L^4Ag](PF_6) (**8**). Particularly, the selective recognition of Ag^+ using organometallic complex containing I-donar (**4**) as a host compound was investigated on the basis of fluorescent and UV/vis spectroscopic titrations.

Results and discussion

Synthesis and general characterization of precursors $L^1H_2\cdot(PF_6)_2$, $L^2H_2\cdot(PF_6)_2$, $L^4H_2\cdot(PF_6)_2$-$L^6H_2\cdot(PF_6)_2$, $L^2H_2\cdot I_2$ and $L^3H_2\cdot I_2$

As shown in Scheme 1, 2,3-dihydroxynaphthalene as starting material was reacted with 2-chloroethanol to afford 2,3-bis(2'-hydroxyethoxy)naphthalene, followed by chlorination of hydroxyl groups with thionyl chloride to give 2,3-bis(2'-chloroethoxy)naphthalene. The reaction of 2,3-bis(2'-chloroethoxy)naphthalene with N-R-benzimidazole (R = ethyl, ^{n}propyl, ^{n}butyl or picolyl) or N-R-imidazole (R = ethyl or ^{n}butyl) in the presence of NaI to afford bis-benzimidazolium (or imidazolium) salts $\mathbf{L^1H_2\cdot I_2}$-$\mathbf{L^6H_2\cdot I_2}$, and subsequent anion exchange with ammonium hexafluorophosphate for $\mathbf{L^1H_2\cdot I_2}$, $\mathbf{L^2H_2\cdot I_2}$ and $\mathbf{L^4H_2\cdot I_2}$-$\mathbf{L^6H_2\cdot I_2}$ were carried out in methanol to give $\mathbf{L^1H_2\cdot(PF_6)_2}$, $\mathbf{L^2H_2\cdot(PF_6)_2}$ and $\mathbf{L^4H_2\cdot(PF_6)_2}$-$\mathbf{L^6H_2\cdot(PF_6)_2}$, respectively. These bis-benzimidazolium (or imidazolium) salts are stable to air, heat and moisture. They are soluble in DMSO, CH_3CN or CH_2Cl_2, but insoluble in benzene, diethyl ether and petroleum ether. In the ^1H NMR spectra of the precursors, the imidazole proton signals (NC*H*N) appear at δ = 9.23-9.99 ppm, which are consistent with the chemical shifts of reported benzimidazolium (or imidazolium) salts.[11]

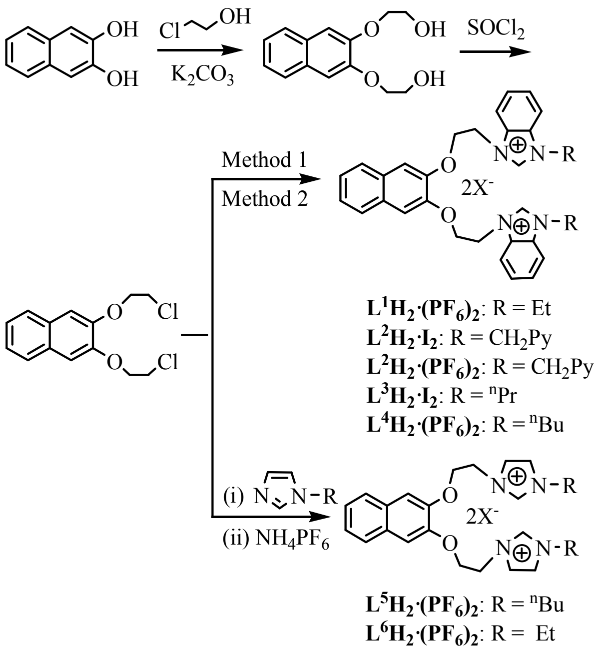

Method 1 for $\mathbf{L^2H_2{\cdot}I_2}$ and $\mathbf{L^3H_2{\cdot}I_2}$, THF, NaI, reflux.
Method 2 for $\mathbf{L^1H_2{\cdot}(PF_6)_2}$, $\mathbf{L^2H_2{\cdot}(PF_6)_2}$ and $\mathbf{L^4H_2{\cdot}(PF_6)_2}$,
(i) THF, NaI, reflux; (ii) the anionic exchange with NH_4PF_6.

Scheme 1 Preparation of precursors

Synthesis and general characterization of anionic complex 1 and NHC metal complexes 2-8

As shown in Scheme 2, the anionic complex $[L^1H_2](Pd_2Cl_6)$ (**1**) was obtained via the reaction of $\mathbf{L^1H_2{\cdot}(PF_6)_2}$ with $PdCl_2$ in CH_3NO_2. The precursors $\mathbf{L^2H_2{\cdot}I_2}$, $\mathbf{L^3H_2{\cdot}I_2}$, $\mathbf{L^4H_2{\cdot}(PF_6)_2}$, $\mathbf{L^5H_2{\cdot}(PF_6)_2}$ or $\mathbf{L^6H_2{\cdot}(PF_6)_2}$ were reacted with $HgCl_2$ or HgI_2 in the presence of KO^tBu in CH_3CN/DMSO to afford complexes $[(L^2HgI)_2Cl]I$ (**2**), $[L^3Hg(HgCl_2I_2)]$ (**3**), $[L^4HgI_2]$ (**4**), $[L^5HgI_2]$ (**5**) and $[L^6Hg(HgI_4)(DMSO)]$ (**6**), respectively. The reaction of $\mathbf{L^2H_2{\cdot}(PF_6)_2}$ or $\mathbf{L^4H_2{\cdot}(PF_6)_2}$ with Ag_2O in $ClCH_2CH_2Cl$/DMSO afforded complexes $[L^2Ag](PF_6)$ (**7**) and $[L^4Ag](PF_6)$ (**8**), respectively. Complexes **1-8** are stable toward air and moisture, soluble in acetonitrile and DMSO, and insoluble in diethyl ether and hydrocarbon solvents. The structures of complexes **1-8** were confirmed by ^1H NMR and ^{13}C NMR spectroscopy and X-ray crystallography. The ^1H NMR and ^{13}C NMR spectra of anionic complex **1** are similar to that of corresponding precursor $\mathbf{L^1H_2{\cdot}(PF_6)_2}$. In the ^1H NMR spectra of **2-8**, the resonances for the benzimidazolium (or imidazolium) protons (NC*H*N) have disappeared, which shows the formation of the expected metal carbene complexes. The chemical shifts of other protons are similar to those of the corresponding precursors. In ^{13}C NMR spectra, the signals for the carbene carbons of complexes **2-6** appear at 175.7-185.6 ppm, which are similar to known carbene metal complexes.[12] The signals of the carbene carbons for silver(I) complexes **7** and **8** were not observed. The absence of the carbene carbon resonance is not usual, and this phenomenon has been reported for some silver(I)-carbene complexes, which may result from the fluxional behaviour of the NHC complexes.[9]

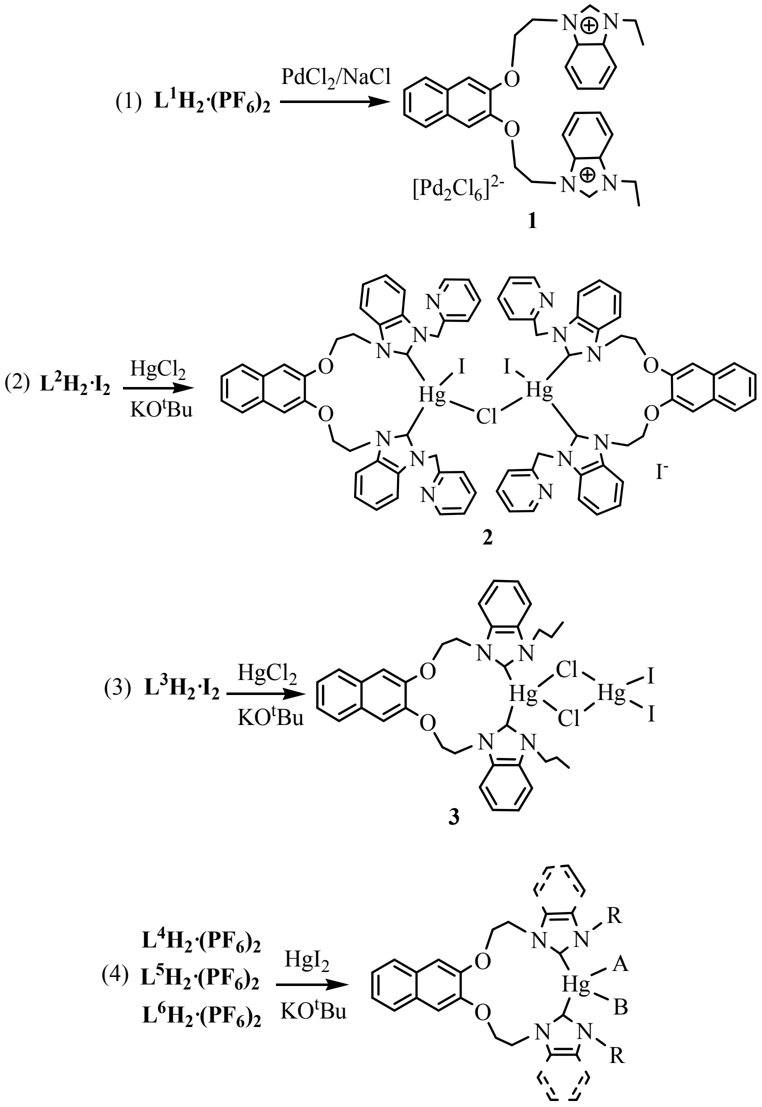

4: bimi, R = ^{n}Bu, A = I, B = I
5: imi, R = ^{n}Bu, A = I, B = I
6: imi, R = Et, A = $[HgI_4]$,
B = $(CH_3)_2SO$

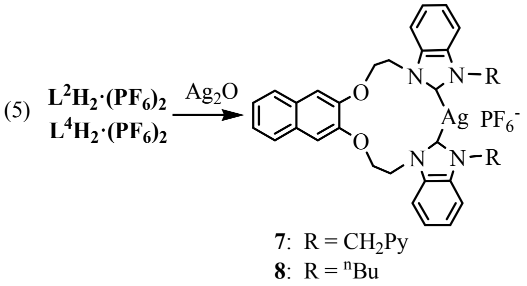

Scheme 2 Preparation of complexes **1-8**

Structure of complexes 1-8

In the cationic unit of complex **1** (Fig. 1), two benzimidazole rings point to opposite directions, and π-π interactions between these two benzimidazole rings are observed (the inter-planar separation being 3.483(8) Å and the center-to-center separation being 3.594(1) Å).[13] Two ethyl groups point to the same direction. The dihedral angles between naphthalene ring and two benzimidazole rings are 40.0(3)° and 38.3(2)°, respectively. The bond angles of N(1)-C(9)-N(2) is 110.6(3)°. In the anionic unit of **1**, the coplanar $[Pd_2Cl_6]^{2-}$ unit is formed by two palladium(II) ions and six chlorine atoms (two bridging chlorine atoms Cl(3) and Cl(4), and four terminal chlorine atoms Cl(1), Cl(2), Cl(5) and Cl(6)). Four atoms Pd(1), Cl(3), Pd(2) and Cl(4) form a parallelogram, in which the bond angles of Cl(3)-Pd(1)-Cl(4) and Pd(1)-Cl(3)-Pd(2) are 85.9(3)° and 94.5(3)°, respectively. The distance of $Pd\text{-}Cl_{terminal}$ (2.270(8) Å) is slightly shorter than that of $Pd\text{-}Cl_{bridging}$ (2.351(8) Å). These values are similar to those of known complexes.[14]

In complexes **2-8** (Fig. 2-Fig. 8), the internal ring angles (N-C-N) at the carbene center are from 105.3(4)° to 107.6(6)°, which are similar to those of known NHC metal complexes,[15, 16] but less than corresponding value in **1** (110.6(3)°). In the same ligand of complexes **2-8**, the dihedral angles between two benzimidazole (or imidazole) rings are from 50.6(4)° to 59.0(9)°, and the naphthalene ring and two benzimidazole (or imidazole) rings formed the dihedral angles of 68.9(6)-87.4(5)° (Table S4 in Supporting Information).

In complexes **3**-**8**, each molecule contains a 13-membered macrometallocycle formed via one bidentate carbene ligand (**L**^{3} for **3**, **L**^{4} for **4** and **8**, **L**^{5} for **5**, **L**^{6} for **6**, **L**^{2} for **7**) and one metal ion (Hg(II) ion for **3**-**6** and Ag(I) for **7** and **8**). In complexes **2**-**6**, each Hg(1) ion was tetra-coordinated with two carbene carbon atoms and two heteroatoms (one iodine atom and one chlorine atom for **2**, two chlorine atoms for **3**, two iodine atoms for **4** and **5**, and one iodine atom and one oxygen atom from DMSO for **6**) to adopt a slightly distorted tetrahedral geometry. In each NHC-Hg-NHC unit of **2**-**6**, two benzimidazole rings form the dihedral angles of 50.6(4)-59.0(9)°. In complexes **2**-**6**, the bond angles of C-Hg-C are from 146.6(3)° to 170.5(3)° and the bond distances of Hg-C are from 2.067(6) Å to 2.146(7) Å. In dinuclear mercury complexes **2**, **3** and **6**, the Hg(1)···Hg(2) separations are 5.344(1) Å , 4.082(6) Å and 4.997(4) Å, respectively, which indicates no interactions between two mercury ions[17] (van der Waals Radii of mercury = 1.70 Å). In complexes **2**, **3**, **5** and **8**, an inversion center in each molecule is observed.

Interestingly, two 13-membered macrometallocycles in **2** (Fig. 2) are connected together via one bridging chlorine atom, in which each macrometallocycle is formed by one bidentate carbene ligand (**L**^{2}) and one Hg(II) ion. The bond distances of Hg(1)-I(1) and Hg(1)-Cl(1) are 3.103(6) Å and 2.878(8) Å, respectively. The bond angles of Hg(1)-Cl(1)-Hg(1A) and I(1)-Hg(1)-Cl(1) are 136.4(6)° and 96.3(1)°, respectively.[15] The dihedral angles between benzimidazole rings and adjacent pyridine rings are from 79.2(7)° to 82.6(1)°.

In **3** (Fig. 3), a coplanar quadrangle $[Hg_2Cl_2]^{2-}$ was formed by Hg(1), Cl(1), Hg(2) and Cl(1A). The bond angles of Cl(1)-Hg(1)-Cl(1A), I(1)-Hg(2)-I(1A) and Hg(1)-Cl(1)-Hg(2) are 79.9(9)°, 125.2(5)° and 95.5(6)°, respectively. The Hg(2) is tetra-coordinated with two iodine atoms and two chlorine atoms. The bond distance of Hg(2)-Cl(1) (2.635(2) Å) is slightly shorter than that of Hg(1)-Cl(1) (2.876(2) Å). The bond distance of Hg(2)-I(1) (2.670(9) Å) is fall within the normal range.[15] The bond angles of Cl-Hg(2)-I are from 104.3(6)° to 114.1(5)°.

In complexes **4** and **5** (Fig. 4 and Fig. 5), the bond distances of Hg-I are from 3.047(5) Å to 3.179(9) Å, and these values are longer than normal values of 2.7-2.8

Å.[12] The bond angles of I-Hg-I are for **4** 101.7(3)° and 94.6(2)° for **5**. The bond angles of C-Hg-I are from 83.5(1)° to 111.5(1)°. These values are similar to those of known NHC-mecury(II) complexes.[15]

In **6**, Hg(2) is surrounded by four iodine atoms to adopt a tetrahedral geometry, in which the bond distances of Hg-I range from 2.752(6) Å to 2.841(5) Å, and the bond angles of I-Hg-I range from 105.0(1)° to 115.9(2)°. These values fall within the normal range.[16] The bond distance of Hg(1)-I(1) (3.363(5) Å) is longer than above mentioned normal values. The bond angles of Hg(1)-I(1)-Hg(2) and Hg(1)-O(3)-S(1) are 106.9(1)° and 119.8(6)°, respectively.

Complexes **7** and **8** have similar structures (Fig. 7 and Fig. 8), in which each silver(I) ion is di-coordinated with two carbene carbon atoms to adopt an approximately linear geometry. The bond angles of C-Ag-C are 171.5(1)° for **7** and 172.1(1)° for **8**, and the bond distances of Ag-C are from 2.086(4) Å to 2.097(3) Å. These values are similar to those of known NHC-silver(I) complexes.[16] In each NHC-Ag-NHC unit of **7** and **8**, two benzimidazole rings form the dihedral angles of 52.1(2)° for **7** and 56.9(1)° for **8**. In complex **7**, the dihedral angles between benzimidazole rings and the adjacent pyridine rings are 79.6(1)° and 83.5(5)°, respectively, and two pyridine rings form the dihedral angle of 33.4(4)°.

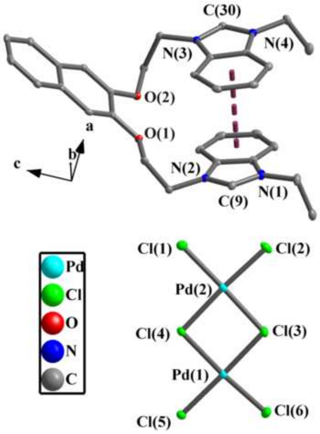

Fig. 1 Perspective view of **1** and anisotropic displacement parameters depicting 30% probability. All hydrogen atoms were omitted for clarity. Selected bond lengths (Å) and angles (°): Pd(1)-Cl(3) 2.318(8), Pd(1)-Cl(4) 2.351(8), Pd(1)-Cl(5) 2.280(8), Pd(1)-Cl(6) 2.277(9), Pd(2)-Cl(1) 2.277(8), Pd(2)-Cl(2) 2.270(8), Pd(2)-Cl(3)

2.328(9), Pd(2)-Cl(4) 2.345(8); Cl(1)-Pd(2)-Cl(2) 90.8(3), Cl(3)-Pd(1)-Cl(4) 85.9(3), Pd(1)-Cl(3)-Pd(2) 94.5(3), N(1)-C(9)-N(2) 110.6(3), N(3)-C(30)-N(4) 110.9(3).

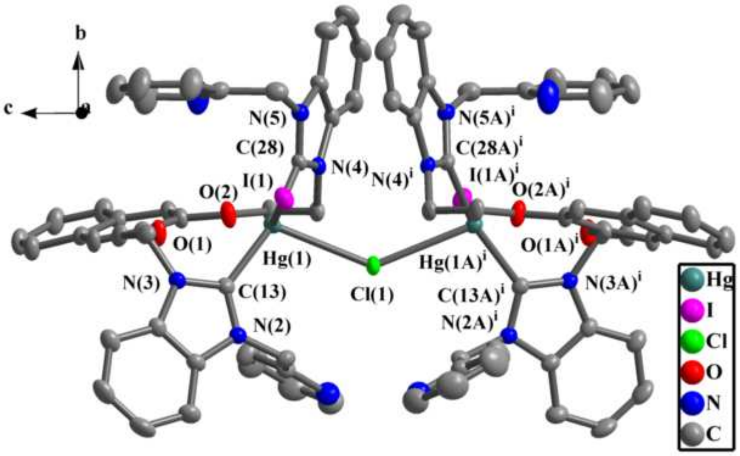

Fig. 2 Perspective view of **2** and anisotropic displacement parameters depicting 30% probability. All hydrogen atoms were omitted for clarity. Selected bond lengths (Å) and angles (˚): C(13)-Hg(1) 2.103(4), C(28)-Hg(1) 2.103(4), Hg(1)-I(1) 3.103(6), Hg(1)-Cl(1) 2.878(8); C(13)-Hg(1)-C(28) 160.2(1), C(13)-Hg(1)-I(1) 86.8(1), C(28)-Hg(1)-I(1) 108.1(1), I(1)-Hg(1)-Cl(1) 96.3(1), Hg(1)-Cl(1)-Hg(1A) 136.4(6), N(2)-C(13)-N(3) 107.0(3), N(4)-C(28)-N(5) 107.5(4). Symm. Code: i: 1 - *x*, *y*, 1.5 - *z*.

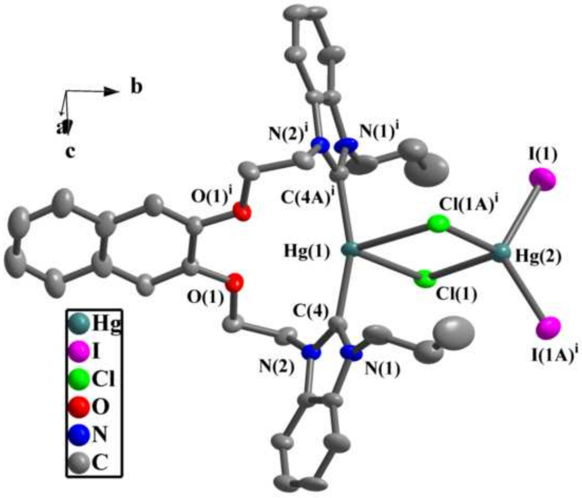

Fig. 3 Perspective view of **3** and anisotropic displacement parameters depicting 30% probability. All hydrogen atoms were omitted for clarity. Selected bond lengths (Å) and angles (˚): Hg(1)-C(4) 2.095(8), Hg(1)-Cl(1) 2.876(2), Hg(2)-I(1) 2.679(9), Hg(2)-Cl(1) 2.635(2); C(4)-Hg(1)-C(4A) 160.8(5), C(4)-Hg(1)-Cl(1) 86.9(2), C(4)-Hg(1)-Cl(1A) 108.1(2), Cl(1)-Hg(2)-I(1) 104.3(6), Cl(1)-Hg(2)-I(1A) 114.1(5),

Cl(1)-Hg(1)-Cl(1A) 79.9(9), I(1)-Hg(2)-I(1A) 125.2(5), Hg(1)-Cl(1)-Hg(2) 95.5(6), N(1)-C(4)-N(2) 107.0(7). Symm. Code: i: 1 - *x*, *y*, 1.5 - *z*.

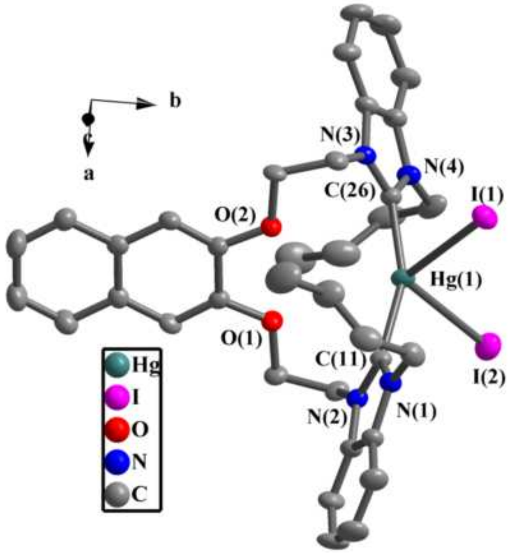

Fig. 4 Perspective view of **4** and anisotropic displacement parameters depicting 30% probability. All hydrogen atoms were omitted for clarity. Selected bond lengths (Å) and angles (˚): Hg(1)-C(11) 2.138(7), Hg(1)-C(26) 2.146(7) Hg(1)-I(1) 3.179(9), Hg(1)-I(2) 3.167(9); C(11)-Hg(1)-C(26) 157.8(3), C(11)-Hg(1)-I(1) 110.4(2), C(11)-Hg(1)-I(2) 83.5(1), C(26)-Hg(1)-I(1) 84.9(2), I(1)-Hg(1)-I(2) 101.7(3), N(1)-C(11)-N(2) 107.3(6), N(3)-C(26)-N(4) 107.6(6).

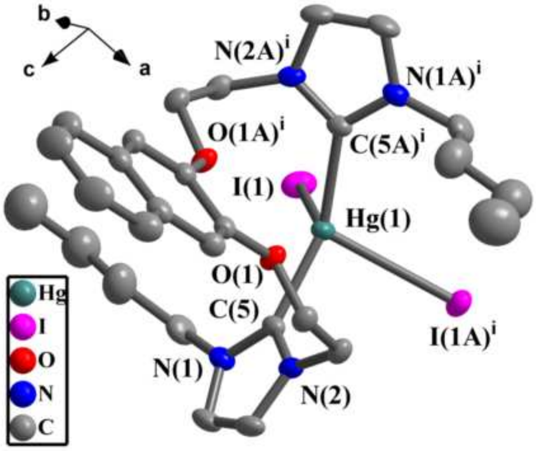

Fig. 5 Perspective view of **5** and anisotropic displacement parameters depicting 30% probability. All hydrogen atoms were omitted for clarity. Selected bond lengths (Å) and angles (˚): Hg(1)-C(5) 2.133(5), Hg(1)-I(1) 3.047(5); C(5)-Hg(1)-C(5A) 146.6(3),

C(5)-Hg(1)-I(1) 91.2(1), C(5)-Hg(1)-I(1A) 111.5(1), I(1)-Hg(1)-I(1A) 94.6(2), N(1)-C(5)-N(2) 105.3(4). Symm. Code: i: - *x*, *y*, 0.5 - *z*.

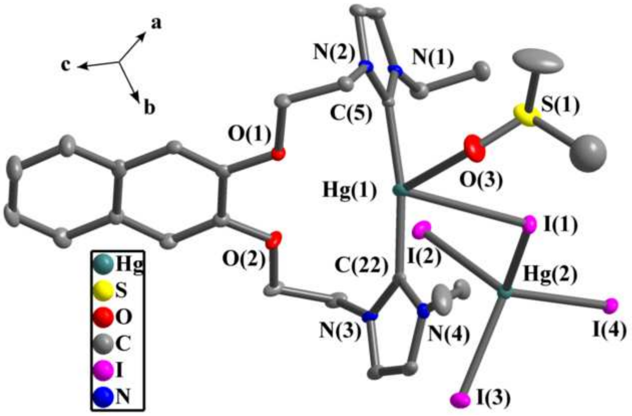

Fig. 6 Perspective view of **6** and anisotropic displacement parameters depicting 30% probability. All hydrogen atoms were omitted for clarity. Selected bond lengths (Å) and angles (˚): Hg(1)-C(5) 2.067(6), Hg(1)-C(22) 2.068(7), Hg(1)-O(3) 2.745(7), Hg(2)-I(2) 2.752(6), Hg(2)-I(3) 2.774(6), Hg(2)-I(4) 2.790(5), Hg(2)-I(1) 2.841(5), Hg(1)-I(1) 3.363(5); C(5)-Hg(1)-C(22) 170.5(3), C(5)-Hg(1)-I(1) 107.5(1), C(22)-Hg(1)-I(1) 81.0(1), C(5)-Hg(1)-O(3) 80.8(4), C(22)-Hg(1)-O(3) 105.0(4) Hg(1)-I(1)-Hg(2) 106.9(1), Hg(1)-O(3)-S(1) 119.8(6), N(1)-C(5)-N(2) 106.0(5), N(3)-C(22)-N(4) 106.1(6).

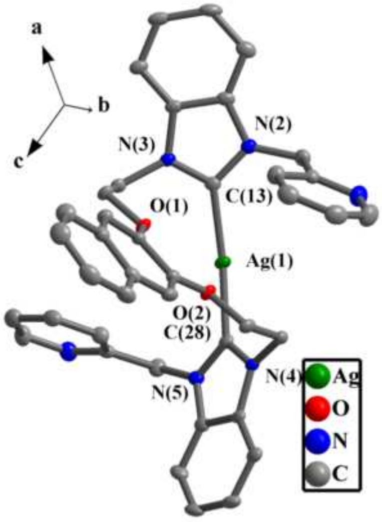

Fig. 7 Perspective view of **7** and anisotropic displacement parameters depicting 30% probability. All hydrogen atoms were omitted for clarity. Selected bond lengths (Å)

and angles (˚): C(13)-Ag(1) 2.086(4), C(28)-Ag(1) 2.094(4); C(13)-Ag(1)-C(28) 171.5(1), N(2)-C(13)-N(3) 105.7(3), N(4)-C(28)-N(5) 106.3(3).

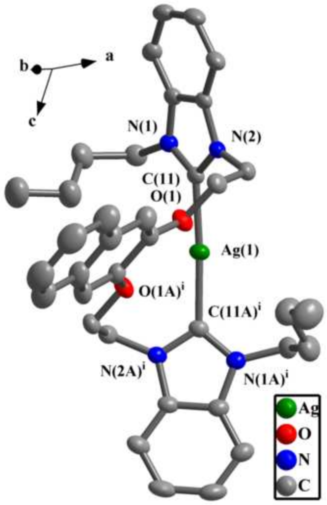

Fig. 8 Perspective view of **8** and anisotropic displacement parameters depicting 30% probability. All hydrogen atoms were omitted for clarity. Selected bond lengths (Å) and angles (˚): C(11)-Ag(1) 2.097(3); C(11)-Ag(1)-C(11A) 172.1(1), N(1)-C(11)-N(2) 106.0(3). Symm. Code: i: 1 - *x*, *y*, 0.5 - *z*.

The crystal packings of complexes 1-8

2D supramolecular layer of **1** is formed via C-H···Cl hydrogen bonds[18] and π-π stacking interactions[15] from benzimidazole rings and naphthalene rings (Fig. S1 in Supporting Information). In the C-H···Cl hydrogen bonds, the hydrogen atoms are from benzimidazole rings. The data of π-π stacking interactions and hydrogen bonds are given in Table S5 and Table S6 in supporting infomation, respectively.

In the crystal packing of **2**, 2D supramolecular layer (Fig. S2(a)) is formed through π-π stacking interactions from benzimidazole rings and C-H···π contacts[19] (the data of C-H···π contacts being given in Table S5). In the C-H···π contacts, the hydrogen atoms are from benzimidazole rings and π systems are from naphthalene rings. Additionally, 3D supramolecular architecture (Fig. S2(b)) is formed through new C-H···π contacts. In new C-H···π contacts, the hydrogen atoms are from pyridine rings and π systems are from benzimidazole rings.

1D chain of **3** is formed via π···π stacking interactions from benzimidazole rings (Fig. S3). 2D supramolecular layer of **4** is formed through π-π stacking interactions from benzimidazole rings and C-H···π contacts (Fig. S4). In the C-H···π contacts, the hydrogen atoms are from CH_3 and π systems are from benzimidazole rings.

In the crystal packing of **5**, 2D supramolecular layer (Fig. S5(a)) is formed through π-π stacking interactions from imidazole rings and C-H···π contacts. In C-H···π contacts, the hydrogen atoms are from CH_2 of ^{n}butyl and π systems are from naphthalene rings. Additionally, 2D layers are further extended 3D supramolecular architecture (Fig. S5(b)) via the same C-H···π contacts.

1D polymeric chain of **6** is formed via C-H···π contacts (Fig. S6). In C-H···π contacts, the hydrogen atoms are from CH_3 and π systems are from imidazole rings.

In the crystal packing of **7**, 2D supramolecular layer (Fig. S7(a)) is formed via π-π stacking interactions from benzimidazole rings and C-H···π contacts. In the C-H···π contacts, the hydrogen atoms are from CH_2 and π systems are from naphthalene rings. 2D supramolecular layers are further extended into 3D supramolecular architecture via another π-π interactions from benzimidazole rings (Fig. S7(b)).

As shown in Fig. S8(a), 2D supramolecular layer of **8** is formed through C-H···π contacts and π-π stacking interactions from benzimidazole rings. In the C-H···π contacts, the hydrogen atoms are from CH_3 and π systems are from benzimidazole rings. Besides, 3D supramolecular architecture (Fig. S8(b)) is formed through the same C-H···π contacts and π-π interactions.

Recognition of Ag^+ using 4 as a host compound

The selective recognition of some cations (Li^+, Na^+, NH_4^+, Ag^+, Ca^{2+}, Co^{2+}, Ni^{2+}, Cu^{2+}, Zn^{2+}, Cd^{2+}, Cr^{3+}, Al^{3+}, Pb^{2+} and Hg^{2+}, and use of their nitrate salts) using **4** as a host compound was investigated by fluorescent and UV/vis titrations in CH_3OH at 25 ˚C. The host compound **4** showed a weak fluorescence emission band at 300 nm to 365 nm (λ_{ex} = 283 nm, the excitation and emission slit: 3 nm and 3 nm), and its fluorescence was not influenced obviously by the addition of 30 equiv of Li^+, Na^+, NH_4^+, Ca^{2+}, Co^{2+}, Ni^{2+}, Cu^{2+}, Zn^{2+}, Cd^{2+}, Cr^{3+}, Al^{3+}, Pb^{2+} and Hg^{2+}, respectively (Fig. 9). Upon addition of Ag^+, the host **4** exhibited a prominent fluorescence enhancement (free **4** of 10 fold) accompanied by a red shift of 14 nm, and these changes are attributed to the internal charge transfer (ICT) process induced by Ag^+.[2(d), 20]

In UV/vis experiments (Fig. S9), upon addition of Ag^+ to the solution of **4**, the absorption around 247 nm to 500 nm increased obviously, but other cations had not obvious effect on the absorption of **4**. Therefore, complex **4** can be functioned as a highly selective host compound for recognition of Ag^+.

In the fluorescent titration experiments (Fig. 10), upon the titration of Ag^+ into solution of **4**, the fluorescence intensity of **4** at 316-394 nm increases gradually with the concentration of Ag^+ increases. In the insets of Fig. 10, the fluorescence intensity at 338 nm shows zigzag enhancement with the increase of concentration of Ag^+ (for more information see Fig. S13 in Supporting Information). In the range of low concentration of Ag^+ (the ratio of C_{Ag+} with $C_{\mathbf{4}}$ being below 0.11), the fluorescence intensity increases slowly. Following gradual increase of concentration of Ag^+, the fluorescence intensity of **4** is sharply enhanced. When the ratio of C_{Ag+} with $C_{\mathbf{4}}$ exceeded 50, higher concentrations of Ag^+ do not lead to further enhancement of fluorescence intensity. The stability constant is calculated as 5.75×10^4 (R = 0.999) for $\mathbf{4}\cdot Ag^+$ by using the equation (1) in CH_3OH at 25 °C.[10(b)]

$$F = F_0 + \frac{F_{max} - F_0}{1+e^{-(\ln Ks+X)}} \quad (1)$$

where F and F_0 are the fluorescence intensity of **4** in the presence and absence of Ag^+, F_{max} is final fluorecence intensity in titration experiment, X means $\ln C_{Ag}{}^+$, and K_S is the stability constant.

In UV/vis titration experiments (Fig. 11), the UV/vis absorption spectra of **4** decreased gradually with the increase of the molar fraction of Ag^+. It is notable that a 1:1 complexation stoichiometry for $\mathbf{4}\cdot Ag^+$ was established by Job's plot analysis at 275 nm (inset of Fig. 11),[21] where the products ($\chi\Delta A$) between molar fractions and the discrepancy of the absorption bands were plotted against molar fractions (χ) of **4** under the conditions of a constant total concentration. When the molar fractions of **4** was 0.5, the $\chi\Delta A$ values for $\mathbf{4}\cdot Ag^+$ reach maximum.[22] The stability constant K for $\mathbf{4}\cdot Ag^+$ calculated from the plot of $A_0/\Delta A$ versus $\mathbf{4}\cdot Ag^+$ based on the standard

Benesi-Hildebrand equation (2) is 1.02 × 10^4 (R = 0.999) in CH_3OH at 25 ˚C (Fig. S10).

$$A_0/(A_0-A) = \{\varepsilon_r/(\varepsilon_r-\varepsilon_c)\}(1/KC_{Ag^+} + 1) \quad (2)$$

where A_0 is the absorption of host **4** in the absence of Ag^+, and A_0-A is the discrepancy of absorption between the absence and presence of Ag^+; ε_r and ε_c are the molar extinction coefficients of **4** and **4**·Ag^+, respectively; C_{Ag^+} is the concentration of Ag^+. The stability constant K is given by the ratio of intercept/slope.[23]

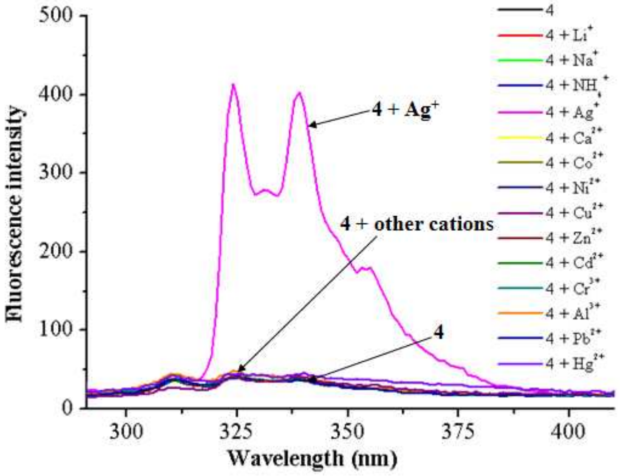

Fig. 9 Fluorescence spectra of **4** (1 × 10^{-5} mol/L) and upon the addition of salts (30 equiv) of Li^+, Na^+, NH_4^+, Ag^+, Ca^{2+}, Co^{2+}, Ni^{2+}, Cu^{2+}, Zn^{2+}, Cd^{2+}, Cr^{3+}, Al^{3+}, Pb^{2+} and Hg^{2+} in CH_3OH at 25 ˚C.

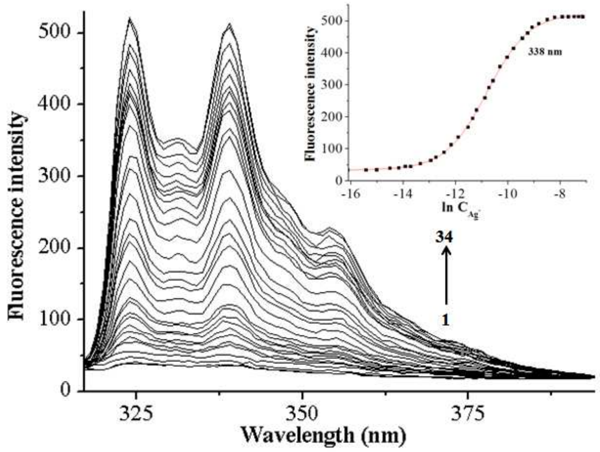

Fig. 10 Fluorescence titration spectra of **4** (1.0 × 10^{-5} mol/L) in the presence of different concentrations of Ag^+ in CH_3OH at 25 ˚C. C_{Ag^+} for curves 1-34 (from

bottom to top) are 0, 0.01, 0.02, 0.03, 0.05, 0.07, 0.09, 0.11, 0.17, 0.25, 0.43, 0.67, 1, 1.5, 2, 3, 5, 7, 9, 13, 17, 21, 25, 30, 35, 40, 45, 50, 55, 60, 65, 70, 75, 80 × 10^{-5} mol/L (λ_{ex} = 283 nm). Inset: the fluorescence at 338 nm of **4** as a function of Ag^+ concentration.

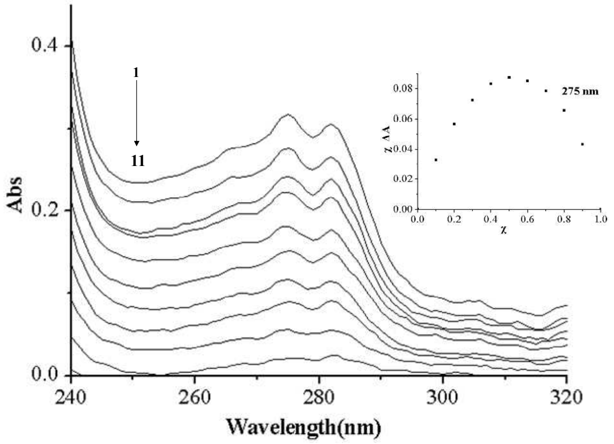

Fig. 11 UV/vis absorption spectra of **4** (2.0 × 10^{-5} mol/L) in CH_3OH at 25 °C. The concentrations of Ag^+ for curves 1-11 (from top to bottom) are: 0, 0.2, 0.4, 0.6, 0.8, 1.0, 1.2, 1.4, 1.6, 1.8, 2 × 10^{-5} mol/L. Inset: The Job plot for **4**·Ag^+ complex at 275 nm.

From the changes in Ag^+-dependent fluorescence intensity (Fig. S11), the detection limit was estimated to be 1.7 × 10^{-8} mol/L for **4**. In reported host compounds for the recognition of Ag^+, their detection limits are in the range of 10^{-5}-10^{-8} M^{-1}.[2(c), 5(n), 24] Our result is similar to the best of them (5.2 × 10^{-8}).

In order to further explore the special selective ability of **4** as a host compound for Ag^+, the competition experiments were conducted. The host **4** (1 × 10^{-5} mol/L) is firstly mixed with 30 equiv of various cations (Li^+, Na^+, NH_4^+, Ca^{2+}, Co^{2+}, Ni^{2+}, Cu^{2+}, Zn^{2+}, Cd^{2+}, Cr^{3+}, Al^{3+}, Pb^{2+} and Hg^{2+}), and then 30 equiv of Ag^+ was added. The fluorescent spectra are exploited to monitor the competition events. As displayed in Fig. S12, only Pb^{2+}, Hg^{2+} and Cu^{2+} cause the fluorescence intensity decreased about 16-25% compared with that in the presence of Ag^+ alone. The fluorescence intensities of other cations are almost identical with that in the presence of Ag^+ alone. The results show that host **4** can discriminate between Ag^+ and other cations.

Interactions of Ag^+ with 4

From the structure of **4** (Fig. 4), we can see that the iodine atoms, oxygen atoms and π system are the most likely binding sites for Ag^+. The possible interactions of Ag^+ with **4** include Ag···I interactions, Ag···O interactions and Ag···π interactions. To obtain detailed information on the binding mode of **4** with Ag^+, ^1H NMR titration experiments were carried out in DMSO-d_6. The spectral differences are depicted in Fig. 12. *H*g was downfield shifted by only 0.04 ppm upon addition of 2 equiv of Ag^+ (Scheme 3). This result suggests that Ag···O interactions have small possibility, otherwise *H*g should have a larger shift. Additionally, the capture of Ag^+ by **4** via Ag···π interactions has also a small possibility. If Ag^+ is captured via Ag···π interactions, Ag^+ should have still second binding group (e.g. another π moiety or L (L = N, O or S)) because Ag···π interactions are generally sandwich π···Ag···π mode[8(a), 25] or L-Ag···π mode.[26] According to the structure of **4** and the results of UV/vis titration experiments (**4** and Ag^+ being 1:1 complexation in insets of Fig. 11), the capture of Ag^+ by **4** is not likely to form these both modes. Besides, in ^1H NMR titration experiments, the signal of protons in benzimidazole and naphthalene were downfield shifted by only 0.03-0.04 ppm upon addition of 2 equiv of Ag^+, which indicates also that the capture of Ag^+ by **4** is not via Ag···π interactions, otherwise the signal of protons in aromatic ring should have a larger shift. Thus, the capture of Ag^+ by **4** should be attributed to Ag···I interactions, and ^1H NMR titration experiments support the conclusion. *H*f and *H*a have relatively large shifts following the addition of Ag^+ (*H*f was downfield shifted by 0.10 ppm and *H*a was upfield shifted by 0.11 ppm upon addition of 2 equiv of Ag^+), which are attributed to the electron-withdrawing effect of Ag^+.

To further understand the complexation behavior of **4** and Ag^+, the infrared spectra (IR) of **4** and **4**·$AgNO_3$ were measured. In the infrared spectra (Fig. S14), we observed that the ν(C-N) absorption bands move from 1168 cm^{-1} in free **4** to 1173 cm^{-1} in **4**·Ag^+.

By comprehensive analysis of the structure of **4**, ^1H NMR spectra and infrared spectra, we can see that the binding force of **4** and Ag^+ originates mainly from Ag···I interactions due to strong affinity of iodine toward Ag^+. When Ag^+ is bound by iodine, the electron-withdrawing effect of Ag^+ leads to the internal charge transfer (ICT). As a result, the fluorescence intensity of **4** enhances remarkably and has a red shift of 14 nm. Similar the internal charge transfer (ICT) process has been reported by Kim.[20(a), (b)]

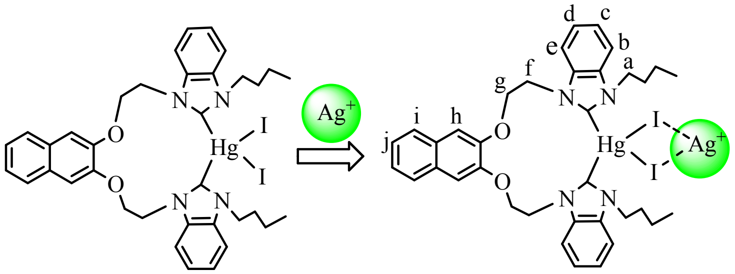

Scheme 3 The interactions of Ag^+ with **4**

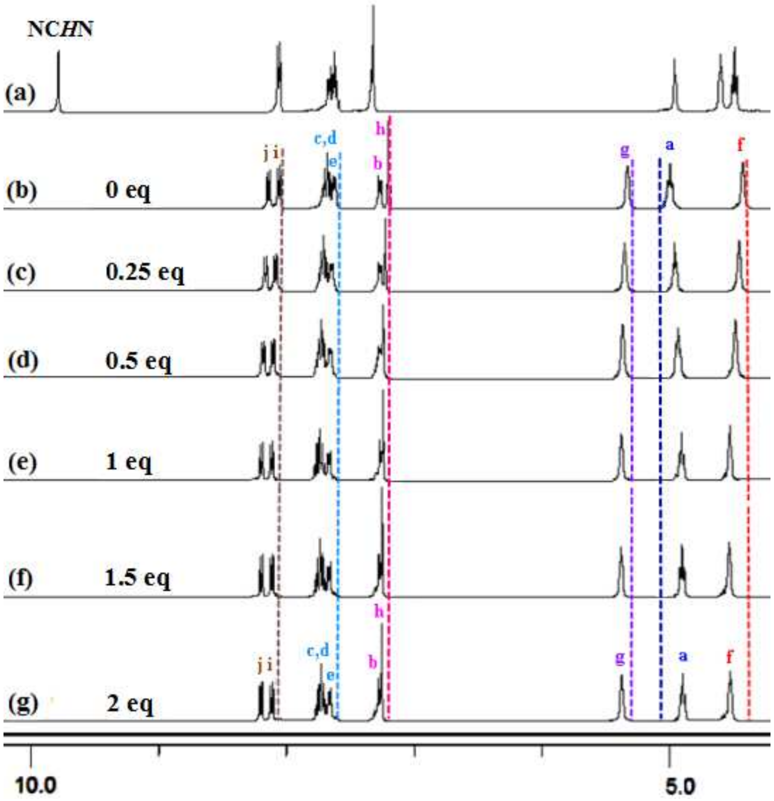

Fig. 12 Partial ^1H NMR spectra in DMSO-d_6. (a) **$L^4H_2\cdot(PF_6)_2$**; (b) complex **4** only; (c) **4** and 0.25 equiv of $AgNO_3$; (d) **4** and 0.5 equiv of $AgNO_3$; (e) **4** and 1 equiv of $AgNO_3$; (f) **4** and 1.5 equiv of $AgNO_3$; (g) **4** and 2 equiv of $AgNO_3$.

Conclusions

In summary, a series of bis-benzimidazolium (or bis-imidazolium) salts and their seven N-heterocyclic carbene mercury(II) and silver(I) complexes, as well as one anionic complex have been prepared and characterized. In complex **1**, two benzimidazole rings point to opposite directions, and π-π interactions between these two benzimidazole rings are observed. In complex **2**, two 13-membered macrometallocycles are linked together by one bridging chlorine atom. In complexes **2-8**, each 13-membered macrometallocycle is formed via one bidentate carbene ligand and one metal ion (Hg(II) for **2-6** and Ag(I) for **7** and **8**). In the crystal packings of **1-8**, 1D chains, 2D supramolecular layers and 3D supramolecular frameworks are formed via intermolecular weak interactions, including C-H···Cl hydrogen bonds, π-π interactions and C-H···π contacts. Interestingly, complex **4** was turned out to be high selectivity and sensitivity for Ag^+ detection, and this means **4** can distinguish Ag^+ with other cations by using the methods of fluorescent and UV/vis spectroscopic titrations. Even if the detection limit is down to 1.7×10^{-8} mol/L, the host **4** for Ag^+ detection is also sensitive. The host **4** may have potential applications in environmental science and life science. Further studies on the synthesis and recognition of organometallic complexes from these precursors, as well as analogous precursors are underway.

Experimental section

General procedures

N-^{n}ethylbenzimidazole and N-^{n}butylbenzimidazole were prepared according to the methods of literature reported.[17(a), 19(a)] All manipulations were performed using Schlenk techniques, and solvents were purified by standard procedures. All the reagents for synthesis and analyses were of analytical grade and used without further purification. Melting points were determined with a Boetius Block apparatus. ^{1}H and ^{13}C NMR spectra were recorded on a Varian Mercury Vx 400 spectrometer at 400 MHz and 100 MHz, respectively. Chemical shifts, δ, are reported in ppm relative to the internal standard TMS for both ^{1}H and ^{13}C NMR. *J* values are given in Hz. Elemental analyses were measured using a Perkin-Elmer 2400C Elemental Analyzer.

The fluorescence spectra were performed using a Cary Eclipse fluorescence spectrophotometer. UV-vis spectra were recorded on a JASCO-V570 spectrometer. IR spectra (KBr) were taken on a Bruker Equinox 55 spectrometer.

Synthesis of 2,3-bis(2'-chloroethoxy)naphthalene

Anhydrous K_2CO_3 (34.552 g, 250.0 mmol) was added to a DMF (150 mL) solution of 2,3-dihydroxynaphthalene (10.000 g, 62.5 mmol), and the suspension was stirred for 0.5 h at 60 ˚C in the N_2 atmosphere. Then 2-chloroethanol (20.000 g, 250.0 mmol) was dropped to the above mixture and stirred continually for 24 h at 110 ˚C. The mixture was poured into 500 mL of water and a white powder of 2,3-bis(2'-hydroxyethoxy)naphthalene was obtained by filtration. Yield: 13.965 g (90%). M.p.: 132-134 ˚C. ^{1}H NMR (400 MHz, DMSO-d$_6$): δ 3.82 (t, J = 5.0 Hz, 4H, CH_2), 4.13 (t, J = 5.2 Hz, 4H, CH_2), 4.97 (d, J = 2.0 Hz, 2H, OH), 7.32 (m, 4H, PhH), 7.73 (q, J = 4.0 Hz, 2H, PhH). ^{13}C NMR (100 MHz, DMSO-d$_6$): δ 148.7 (PhC), 128.8 (PhC), 126.1 (PhC), 123.8 (PhC), 107.7 (PhC), 70.0 (OCH$_2$CH$_2$), 59.3 (OCH$_2$$CH_2$).

Thionyl chloride (23.972 g, 201.5 mmol) was added dropwise to the chloroform solution (100 mL) of 2,3-bis(2'-hydroxyethoxy)naphthalene (10.000 g, 40.3 mmol) and pyridine (15.938 g, 201.5 mmol) within 1 h at ambient temperature. The mixture solution was stirred for 12 h at 60 ˚C. The resulting mixture was poured into 300 mL of water, and the water layer was extracted with chloroform (30 mL × 3). The organic layer was combined and dried over anhydrous $MgSO_4$. After removing chloroform, 2,3-bis(2'-chloroethoxy)naphthalene was obtained as a pale yellow powder. Yield: 6.442 g (56%). M.p.: 72-74 ˚C. ^{1}H NMR (400 MHz, CDCl$_3$): δ 3.92 (t, J = 6.0 Hz, 4H, CH_2), 4.40 (t, J = 18.4 Hz, 4H, CH_2), 7.20 (s, 2H, PhH), 7.37 (m, 2H, PhH), 7.69 (m, 2H, PhH). ^{13}C NMR (100 MHz, CDCl$_3$): δ 148.4 (PhC), 129.6 (PhC), 126.4 (PhC), 124.7 (PhC), 110.2 (PhC), 69.3 (OCH$_2$CH$_2$), 41.7 (OCH$_2$$CH_2$).

Preparation of 2,3-bis[2'-(N-ethylbenzimidazoliumyl)ethoxy]naphthalene hexafluorophosphate ($L^1H_2\cdot(PF_6)_2$)

A THF (100 mL) solution of 2,3-bis(2-chloroethoxy)naphthalene (2.000 g, 7.0 mmol), N-ethylbenzimidazole (3.084 g, 21.1 mmol) and NaI (3.164 g, 21.1 mmol) was stirred for 7 days under refluxing, and a yellow oil of 2,3-bis[2'-(N-ethylbenzimidazoliumyl)ethoxy]naphthalene iodide was formed.

NH_4PF_6 (3.000 g, 18.4 mmol) was added to a methanol solution (150 mL) of 2,3-bis[2'-(N-ethylbenzimidazoliumyl)ethoxy]naphthalene iodide (4.638 g, 6.1 mmol) with stirring for 3 days, and a white precipitate was formed. The precipitate was collected by filtration and washed with a small portion of methanol to give 2,3-bis[2-(N'-ethylbenzimidazoliumyl)ethoxy]naphthalene hexafluorophosphate (**$L^1H_2{\cdot}(PF_6)_2$**) as a white powder. Yield: 3.790 g (78%). M.p.: 198-200 ˚C. Anal. Calcd for $C_{32}H_{34}N_4O_2P_2F_{12}$: C, 48.24; H, 4.30; N, 7.03%. Found: C, 48.33 H, 4.54; N, 7.28%. ^{1}H NMR (400 MHz, DMSO-d_6): δ 1.51 (t, J = 7.2 Hz, 6H, C*H*$_3$), 4.51 (m, 4H, C*H*$_2$), 4.60 (m, 4H, C*H*$_2$), 5.03 (m, 4H, C*H*$_2$), 7.35 (m, 4H, Ph*H*), 7.62 (m, 2H, Ph*H*), 7.73 (m, 4H, Ph*H*), 8.05 (m, 4H, Ph*H*), 9.77 (s, 2H, 2-bimi*H*). ^{13}C NMR (100 MHz, DMSO-d_6): δ 147.1 (bimi-N*C*N), 142.3 (Ph*C*), 131.4 (Ph*C*), 130.6 (Ph*C*), 128.8 (Ph*C*), 126.4 (Ph*C*), 126.3 (Ph*C*), 126.2 (Ph*C*), 124.5 (Ph*C*), 114.0 (Ph*C*), 113.4 (Ph*C*), 108.5 (Ph*C*), 66.2 (O*C*H$_2$CH$_2$), 46.2 (OCH$_2$*C*H$_2$), 42.0 (*C*H$_2$CH$_3$), 14.1 (CH$_2$*C*H$_3$) (bimi = benzimidazole).

Preparation of 2,3-bis[2'-(N-picolylbenzimidazoliumyl)ethoxy]naphthalene Iodide ($L^2H_2{\cdot}I_2$)

A THF (100 mL) solution of 2,3-bis(2-chloroethoxy)naphthalene (2.000 g, 7.0 mmol), N-picolybenzimidazole (4.414 g, 21.1 mmol) and NaI (3.164 g, 21.1 mmol) was stirred for 7 days under refluxing, and a white precipitate was formed. The precipitate was collected by filtration and washed with THF to give 2,3-bis[2'-(N-picolylbenzimidazoliumyl)ethoxy]naphthalene iodide (**$L^2H_2{\cdot}I_2$**) as a white powder. Yield: 3.667 g (60%). M.p.: 202-204 ˚C. Anal. Calcd for $C_{40}H_{36}N_6O_2I_2$: C, 54.19; H, 4.09; N, 9.47%. Found: C, 54.44; H, 4.38; N, 9.18%. ^{1}H NMR (400 MHz, DMSO-d_6): δ 4.60 (t, J = 4.6 Hz, 4H, C*H*$_2$), 5.03 (t, J = 4.8 Hz, 4H, C*H*$_2$), 5.94 (s, 4H, C*H*$_2$), 7.36 (q, J = 3.9 Hz, 6H, Ar*H*), 7.58 (m, 4H, Ar*H*), 7.70 (m, 4H, Ar*H*), 7.91 (m, 4H, Ar*H*), 8.06 (q, J = 3.1 Hz, 2H, Ar*H*), 8.41 (d, J = 4.8 Hz, 2H, Ar*H*), 9.99 (s, 2H, 2-bimi*H*). ^{13}C NMR (100 MHz, DMSO-d_6): δ 153.3 (bimi-N*C*N), 150.0 (Ar*C*), 147.7 (Ar*C*), 138.0 (Ar*C*), 131.8 (Ar*C*), 131.5 (Ar*C*), 129.3 (Ar*C*), 127.2 (Ar*C*), 126.7

(Ar*C*), 125.0 (Ar*C*), 124.2 (Ar*C*), 123.2 (Ar*C*), 114.6 (Ar*C*), 114.2 (Ar*C*), 109.2 (Ar*C*), 67.4 (O*C*H$_2$CH$_2$), 51.3 (OCH$_2$*C*H$_2$), 49.0 (N*C*H$_2$).

Preparation of 2,3-bis[2'-(N-picolylbenzimidazoliumylethoxy]naphthalene hexafluorophosphate ($L^2H_2\cdot(PF_6)_2$)

This compound was prepared in a manner analogous to that for **$L^1H_2\cdot(PF_6)_2$**, only N-picolylbenzimidazole (4.414 g, 21.1 mmol) was used instead of N-ethylbenzimidazole. Yield: 5.554 g (86%). M.p.: 134-136 ˚C. Anal. Calcd for $C_{40}H_{36}N_6O_2P_2F_{12}$: C, 52.06; H, 3.93; N, 9.10%. Found: C, 52.32; H, 3.77; N, 9.41%. ^{1}H NMR (400 MHz, DMSO-d$_6$): δ 4.60 (d, *J* = 4.4 Hz, 4H, C*H*$_2$), 5.02 (s, 4H, C*H*$_2$), 5.94 (s, 4H, C*H*$_2$), 7.36 (m, 6H, Ar*H*), 7.58 (m, 4H, Ar*H*), 7.70 (m, 4H, Ar*H*), 7.91 (m, 4H, Ar*H*), 8.06 (q, *J* = 3.1 Hz, 2H, Ar*H*), 8.41 (d, *J* = 4.4 Hz, 2H, Ar*H*), 9.99 (s, 2H, 2-bimi*H*). ^{13}C NMR (100 MHz, DMSO-d$_6$): δ 152.8 (bimi-N*C*N), 149.5 (Ar*C*), 147.2 (Ar*C*), 143.4 (Ar*C*), 137.5 (Ar*C*), 131.3 (Ar*C*), 131.0 (Ar*C*), 128.9 (Ar*C*), 126.7 (Ar*C*), 126.4 (Ar*C*), 126.2 (Ar*C*), 124.5 (Ar*C*), 123.7 (Ar*C*), 122.7 (Ar*C*), 114.1 (Ar*C*), 113.7 (Ar*C*), 108.7 (Ar*C*), 66.3 (O*C*H$_2$CH$_2$), 50.8 (OCH$_2$*C*H$_2$), 46.4 (N*C*H$_2$).

Preparation of 2,3-bis[2'-(N-^{n}propylbenzimidazoliumyl)ethoxy]naphthalene iodide ($L^3H_2\cdot I_2$)

This compound was prepared in a manner analogous to that for **$L^2H_2\cdot I_2$**, only N-^{n}propylbenzimidazole (3.380 g, 21.1 mmol) was used instead of N-picolybenzimidazole. Yield: 4.193 g (76%). M.p.: 98-100 ˚C. Anal. Calcd for $C_{34}H_{38}N_4O_2I_2$: C, 51.78; H, 4.85; N, 7.10%. Found: C, 51.48; H, 4.57; N, 7.32%. ^{1}H NMR (400 MHz, DMSO-d$_6$): δ 0.90 (t, *J* = 7.4 Hz, 6H, C*H*$_3$), 1.91 (q, *J* = 7.0 Hz, 4H, C*H*$_2$), 4.49 (t, *J* = 4.6 Hz, 4H, C*H*$_2$), 4.61 (t, *J* = 4.6 Hz, 4H, C*H*$_2$), 4.99 (t, *J* = 4.6 Hz, 4H, C*H*$_2$), 7.34 (m, 4H, Ph*H*), 7.69 (m, 6H, Ph*H*), 8.09 (t, *J* = 4.8 Hz, 4H, Ph*H*), 9.92 (s, 2H, 2-bimi*H*). ^{13}C NMR (100 MHz, DMSO-d$_6$): δ 147.1 (bimi-N*C*N), 142.6 (Ph*C*), 131.3 (Ph*C*), 130.9 (Ph*C*), 128.8 (Ph*C*), 126.5 (Ph*C*), 126.4 (Ph*C*), 126.2 (Ph*C*), 124.4 (Ph*C*), 114.1 (Ph*C*), 113.5 (Ph*C*), 108.5 (Ph*C*), 66.1 (O*C*H$_2$CH$_2$), 48.0 (OCH$_2$*C*H$_2$), 46.3 (*C*H$_2$CH$_2$CH$_3$), 22.0 (CH$_2$*C*H$_2$CH$_3$), 10.5 (CH$_2$CH$_2$*C*H$_3$).

Preparation of 2,3-bis[2'-(N-^{n}butylbenzimidazoliumyl)ethoxy]naphthalene hexafluorophosphate ($L^4H_2\cdot(PF_6)_2$)

This compound was prepared in a manner analogous to that for **L^{1}H$_2$·(PF$_6$)$_2$**, only N-^{n}butylbenzimidazole (3.676 g, 21.1 mmol) was used instead of N-ethylbenzimidazole. Yield: 4.760 g (80%). M.p.: 88-90 ˚C. Anal. Calcd for $C_{36}H_{42}N_4O_2P_2F_{12}$: C, 50.70; H, 4.96; N, 6.57%. Found: C, 50.43; H, 4.72; N, 6.65%. ^{1}H NMR (400 MHz, DMSO-d$_6$): δ 0.89 (t, J = 7.4 Hz, 6H, C*H*$_3$), 1.33 (q, J = 7.6 Hz, 4H, C*H*$_2$), 1.86 (m, 4H, C*H*$_2$), 4.49 (t, J = 7.2 Hz, 4H, C*H*$_2$), 4.60 (t, J = 5.2 Hz, 4H, C*H*$_2$), 4.96 (t, J = 4.4 Hz, 4H, C*H*$_2$), 7.34 (t, J = 4.0 Hz, 4H, Ph*H*), 7.67 (m, 6H, Ph*H*), 8.06 (t, J = 7.6 Hz, 4H, Ph*H*), 9.78 (s, 2H, 2-bimi*H*). ^{13}C NMR (100 MHz, DMSO-d$_6$): δ 147.1 (bimi-N*C*N), 142.5 (Ph*C*), 131.3 (Ph*C*), 130.8 (Ph*C*), 128.8 (Ph*C*), 126.5 (Ph*C*), 126.3 (Ph*C*), 126.2 (Ph*C*), 124.5 (Ph*C*), 114.0 (Ph*C*), 113.5 (Ph*C*), 108.5 (Ph*C*), 66.2 (O*C*H$_2$CH$_2$), 46.4 (OCH$_2$*C*H$_2$), 46.3 (*C*H$_2$CH$_2$CH$_2$CH$_3$), 30.5 (CH$_2$*C*H$_2$CH$_2$CH$_3$), 19.0 (CH$_2$CH$_2$*C*H$_2$CH$_3$), 13.3 (CH$_2$CH$_2$CH$_2$*C*H$_3$).

Preparation of 2,3-bis[2'-(N-^{n}butylimidazoliumyl)ethoxy]naphthalene hexafluorophosphate (L^{5}H$_2$·(PF$_6$)$_2$)

This compound was prepared in a manner analogous to that for **L^{1}H$_2$·(PF$_6$)$_2$**, only N-^{n}butylimidazole (2.619 g, 21.1 mmol) was used instead of N-ethylbenzimidazole. Yield: 4.212 g (80%). M.p.: 112-114 ˚C. Anal. Calcd for $C_{28}H_{38}N_4O_2P_2F_{12}$: C, 44.68; H, 5.08; N, 7.44%. Found: C, 44.78; H, 5.35; N, 7.63%. ^{1}H NMR (400 MHz, DMSO-d$_6$): δ 0.88 (t, J = 7.4 Hz, 6H, C*H*$_3$), 1.27 (m, 4H, C*H*$_2$), 1.78 (m, 4H, C*H*$_2$), 4.21 (t, J = 7.0 Hz, 4H, C*H*$_2$), 4.50 (t, J = 5 Hz, 4H, C*H*$_2$), 4.69 (t, J = 4.6 Hz, 4H, C*H*$_2$), 7.36 (t, J = 3.6 Hz, 4H, Ph*H*), 7.74 (q, J = 3.2 Hz, 2H, Ph*H*), 7.80 (d, J = 1.6 Hz, 2H, imi*H*), 7.81 (d, J = 1.6 Hz, 2H, imi*H*), 9.25 (s, 2H, 2-imi*H*). ^{13}C NMR (100 MHz, DMSO-d$_6$): δ 147.3 (imi-N*C*N), 136.4 (Ph*C*), 128.9 (Ph*C*), 126.3 (Ph*C*), 124.5 (Ph*C*), 123.0 (Ph*C*), 122.3 (Ph*C*), 108.8 (Ph*C*), 66.6 (O*C*H$_2$CH$_2$), 48.6 (OCH$_2$*C*H$_2$), 48.4 (*C*H$_2$CH$_2$CH$_2$CH$_3$), 31.3 (CH$_2$*C*H$_2$CH$_2$CH$_3$), 18.7 (CH$_2$CH$_2$*C*H$_2$CH$_3$), 13.2 (CH$_2$CH$_2$CH$_2$*C*H$_3$) (imi = imidazole).

Preparation of 2,3-bis[2'-(N-ethylimidazoliumyl)ethoxy]naphthalene hexafluorophosphate (L^{6}H$_2$·(PF$_6$)$_2$)

This compound was prepared in a manner analogous to that for **L^{1}H$_2$·(PF$_6$)$_2$**, only N-ethylimidazole (2.028 g, 21.1 mmol) was used instead of N-ethylbenzimidazole.

Yield: 3.508 g (72%). M.p.: 122-124 ˚C. Anal. Calcd for $C_{24}H_{30}N_4O_2P_2F_{12}$: C, 41.38; H, 4.34; N, 8.04%. Found: C, 41.47; H, 4.58; N, 8.31%. ^{1}H NMR (400 MHz, DMSO-d$_6$): δ 1.43 (t, J = 7.2 Hz, 6H, CH_3), 4.25 (q, J = 7.2 Hz, 4H, CH_2), 4.50 (t, J = 4.8 Hz, 4H, CH_2), 4.68 (t, J = 4.6 Hz, 4H, CH_2), 7.37 (q, J = 10.1 Hz, 4H, Ph*H*), 7.75 (q, J = 3.2 Hz, 2H, Ph*H*), 7.77 (s, 2H, imi*H*), 7.82 (s, 2H, imi*H*), 9.23 (s, 2H, 2-imi*H*). ^{13}C NMR (100 MHz, DMSO-d$_6$): δ 147.3 (imi-N*C*N), 136.1 (Ph*C*), 128.9 (Ph*C*), 126.3 (Ph*C*), 124.5 (Ph*C*), 122.9 (Ph*C*), 122.0 (Ph*C*), 108.8 (Ph*C*), 66.6 (O*C*H$_2$CH$_2$), 48.4 (OCH$_2$*C*H$_2$), 44.3 (*C*H$_2$CH$_3$), 15.0 (*C*H$_3$).

Preparation of complexes 1-8

Preparation of [L^{1}H$_2$](Pd$_2$Cl$_6$) (1)

A CH_3NO_2 (15 mL) suspension of **L^{1}H$_2$·(PF$_6$)$_2$** (0.159 g, 0.2 mmol), $PdCl_2$ (0.106 g, 0.6 mmol) and NaCl (0.034 g, 0.6 mmol) was stirred for 24 h under refluxing, and then a yellow solution was formed. The resulting solution was filtered and concentrated to 5 mL, and diethyl ether (5 mL) was added to precipitate a yellow powder. Yield: 0.050 g (27%). M.p.: 196-198 ˚C. Anal. Calcd for $C_{32}H_{34}Cl_6N_4O_2Pd_2$: C, 41.22; H, 3.67; N, 6.01%. Found: C, 41.56; H, 3.41; N, 6.39%. ^{1}H NMR (400 MHz, DMSO-d$_6$): δ 1.50 (s, 6H, CH_3), 4.97 (m, 8H, CH_2), 4.98 (q, J = 1.2 Hz, 4H, CH_2), 7.33 (s, 4H, Ph*H*), 7.62 (t, J = 2.0 Hz, 4H, Ph*H*), 7.68 (t, J = 0.8 Hz, 2H, Ph*H*), 8.05 (m, 4H, Ph*H*), 9.86 (s, 2H, 2-bimiH). ^{13}C NMR (100 MHz, DMSO-d$_6$): δ 147.1 (bimi-N*C*N), 142.5 (Ph*C*), 130.6 (Ph*C*), 128.8 (Ph*C*), 126.4 (Ph*C*), 126.3 (Ph*C*), 126.2 (Ph*C*), 124.4 (Ph*C*), 114.0 (Ph*C*), 113.4 (Ph*C*), 111.0 (Ph*C*), 108.5 (Ph*C*), 66.3 (O*C*H$_2$CH$_2$), 48.5 (OCH$_2$*C*H$_2$), 42.0 (*C*H$_2$CH$_3$), 14.1 (CH$_2$*C*H$_3$).

Preparation of [(L^{2}Hg)$_2$I$_2$Cl]I (2)

An acetonitrile/DMSO (15 mL, v:v = 2:1) suspension of **L^{2}H$_2$·I$_2$** (0.177 g, 0.2 mmol), $HgCl_2$ (0.065 g, 0.2 mmol) and KO^{t}Bu (0.056g, 0.5 mmol) was stirred for 24 h under refluxing, and a yellow solution was formed. The solution was filtered and concentrated to 5 mL, and diethyl ether (5 mL) was added to precipitate a yellow powder. Yield: 0.216 g (26%). Mp: 260-262 ˚C. Anal. Calcd for $C_{160}H_{136}Cl_2Hg_4I_6N_{24}O_8$: C, 46.22 H, 3.29; N, 8.08%. Found: C, 46.47 H, 3.58; N, 8.39%. ^{1}H NMR (400 MHz, DMSO-d$_6$): δ 4.41 (s, 4H, CH_2), 5.33 (s, 4H, CH_2), 6.55

(s, 4H, Ar*H*), 7.32 (m, 6H, Ar*H*), 7.69 (m, 8H, Ar*H*), 7.82 (m, 2H, Ar*H*), 7.92 (d, *J* = 8.0 Hz, 2H, Ar*H*), 8.11 (d, *J* = 8.0 Hz, 2H, Ar*H*), 8.32 (d, *J* = 8.0 Hz, 2H, Ar*H*). ^{13}C NMR (100 MHz, DMSO-d$_6$): δ 185.6 (C_{carbene}), 154.1 (Ar*C*), 149.4 (Ar*C*), 147.2 (Ar*C*), 137.4 (Ar*C*), 133.2 (Ar*C*), 132.1 (Ar*C*), 128.6 (Ar*C*), 126.2 (Ar*C*), 125.7 (Ar*C*), 125.6 (Ar*C*), 124.2 (Ar*C*), 123.4 (Ar*C*), 122.7 (Ar*C*), 113.1 (Ar*C*), 112.8 (Ar*C*), 106.9 (Ar*C*), 65.5 (O*C*H$_2$CH$_2$), 51.7 (OCH$_2$*C*H$_2$), 47.8 (*C*H$_2$).

Preparation of [L^{3}Hg(HgCl$_2$I$_2$)] (3)

This complex was prepared in a manner analogous to that for **2**, only **L^{3}H$_2$·I$_2$** (0.157 g, 0.2 mmol) and HgCl$_2$ (0.130 g, 0.4 mmol) were used instead of **L^{2}H$_2$·I$_2$** and HgCl$_2$ (0.065 g, 0.2 mmol). Yield: 0.075 g (30%). M.p.: 278-280 ˚C. Anal. Calcd for $C_{34}H_{36}Cl_2Hg_2I_2N_4O_2$: C, 32.44; H, 2.88; N, 4.45%. Found: C, 32.56; H, 2.57; N, 4.59%. ^{1}H NMR (400 MHz, DMSO-d$_6$): δ 1.11 (t, *J* = 7.2 Hz, 6H, C*H*$_3$), 1.96 (q, *J* = 7.1 Hz, 4H, C*H*$_2$), 4.41 (s, 4H, C*H*$_2$), 5.00 (t, *J* = 6.8 Hz, 4H, C*H*$_2$), 5.37 (s, 4H, C*H*$_2$), 7.20 (s, 2H, Ph*H*), 7.28 (q, *J* = 3.1 Hz, 2H, Ph*H*), 7.71 (m, 6H, Ph*H*), 8.07 (d, *J* = 7.6 Hz, 2H, Ph*H*), 8.15 (d, *J* = 8.0 Hz, 2H, Ph*H*). ^{13}C NMR (100 MHz, DMSO-d$_6$): δ 184.9 (C_{carbene}), 146.9 (Ph*C*), 132.8 (Ph*C*), 132.2 (Ph*C*), 128.5 (Ph*C*), 126.1 (Ph*C*), 125.78 (Ph*C*), 125.70 (Ph*C*), 124.3 (Ph*C*), 113.3 (Ph*C*), 112.8 (Ph*C*), 106.9 (Ph*C*), 65.3 (O*C*H$_2$CH$_2$), 48.5 (OCH$_2$*C*H$_2$), 47.6 (*C*H$_2$CH$_2$CH$_3$), 23.2 (CH$_2$*C*H$_2$CH$_3$), 15.1 (CH$_2$CH$_2$*C*H$_3$).

Preparation of [L^{4}HgI$_2$] (4)

This complex was prepared in a manner analogous to that for **2**, only **L^{4}H$_2$·(PF$_6$)$_2$** (0.170 g, 0.2 mmol) and HgI$_2$ (0.227 g, 0.5 mmol) were used instead of **L^{2}H$_2$·I$_2$** and HgCl$_2$. Yield: 0.077 g (38%). M.p.: 257-259 ˚C. Anal. Calcd for $C_{36}H_{40}HgI_2N_4O_2$: C, 42.59; H, 3.97; N, 5.51%. Found: C, 42.83; H, 3.65; N, 5.54%. ^{1}H NMR (400 MHz, DMSO-d$_6$): δ 0.87 (t, *J* = 7.4 Hz, 6H, C*H*$_3$), 1.44 (q, *J* = 7.6 Hz, 4H, C*H*$_2$), 1.89 (t, *J* = 7.4 Hz, 4H, C*H*$_2$), 4.39 (s, 4H, C*H*$_2$), 5.07 (d, *J* = 6.4 Hz, 4H, C*H*$_2$), 5.35 (s, 4H, C*H*$_2$), 7.18 (s, 2H, Ph*H*), 7.27 (q, *J* = 3.1 Hz, 2H, Ph*H*), 7.68 (m, 6H, Ph*H*), 8.04 (d, *J* = 7.6 Hz, 2H, Ph*H*), 8.13 (d, *J* = 7.6 Hz, 2H, Ph*H*). ^{13}C NMR (100 MHz, DMSO-d$_6$): δ 185.2 (C_{carbene}), 146.9 (Ph*C*), 132.9 (Ph*C*), 132.0 (Ph*C*), 128.5 (Ph*C*), 126.1 (Ph*C*), 125.6 (Ph*C*), 125.5 (Ph*C*), 124.3 (Ph*C*), 113.2 (Ph*C*), 112.7 (Ph*C*), 106.8 (Ph*C*), 65.2

(O*C*H$_2$CH$_2$), 47.7 (OCH$_2$*C*H$_2$), 47.4 (*C*H$_2$CH$_2$CH$_2$CH$_3$), 32.0 (CH$_2$*C*H$_2$CH$_2$CH$_3$), 19.1 (CH$_2$CH$_2$*C*H$_2$CH$_3$), 13.7 (CH$_2$CH$_2$CH$_2$*C*H$_3$).

Preparation of [L^{5}HgI$_2$] (5)

This complex was prepared in a manner analogous to that for **2**, only **L^{5}H$_2$·(PF$_6$)$_2$** (0.150 g, 0.2 mmol) and HgI$_2$ (0.227 g, 0.5 mmol) were used instead of **L^{2}H$_2$·I$_2$** and HgCl$_2$. Yield: 0.084 g (46%). Mp: 186-188 ˚C. Anal. Calcd for $C_{28}H_{36}HgI_2N_4O_2$: C, 36.75; H, 3.96; N, 6.12%. Found: C, 36.93; H, 3.53; N, 6.47%. ^{1}H NMR (400 MHz, DMSO-d$_6$): *δ* 0.85 (t, *J* = 7.4 Hz, 6H, C*H*$_3$), 1.32 (q, *J* = 7.6 Hz, 4H, C*H*$_2$), 1.82 (m, 4H, C*H*$_2$), 4.33 (t, *J* = 4.2 Hz, 4H, C*H*$_2$), 4.61 (t, *J* = 7.2 Hz, 4H, C*H*$_2$), 4.90 (s, 4H, C*H*$_2$), 7.26 (s, 2H, Ph*H*), 7.34 (q, *J* = 3.1 Hz, 2H, Ph*H*), 7.73 (q, *J* = 3.2 Hz, 2H, Ph*H*), 7.81 (d, *J* = 1.6 Hz, 2H, Ph*H*), 7.86 (d, *J* = 1.6 Hz, 2H, Ph*H*). ^{13}C NMR (100 MHz, DMSO-d$_6$): *δ* 176.6 (C_{carbene}), 147.0 (Ph*C*), 128.6 (Ph*C*), 126.2 (Ph*C*), 124.3 (Ph*C*), 123.7 (Ph*C*), 123.3 (Ph*C*), 106.9 (Ph*C*), 66.8 (O*C*H$_2$CH$_2$), 50.1 (OCH$_2$*C*H$_2$), 49.8 (*C*H$_2$CH$_2$CH$_2$CH$_3$), 32.8 (CH$_2$*C*H$_2$CH$_2$CH$_3$), 18.9 (CH$_2$CH$_2$*C*H$_2$CH$_3$), 13.6 (CH$_2$CH$_2$CH$_2$*C*H$_3$).

Preparation of [L^{6}Hg(HgI$_4$)(DMSO)] (6)

This complex was prepared in a manner analogous to that for **2**, only **L^{6}H$_2$·(PF$_6$)$_2$** (0.139 g, 0.2 mmol) and HgI$_2$ (0.227 g, 0.5 mmol) were used instead of **L^{2}H$_2$·I$_2$** and HgCl$_2$. Yield: 0.097 g (35%). Mp: 154-156 ˚C. Anal. Calcd for $C_{26}H_{34}Hg_2I_4N_4O_3S$: C, 22.44; H, 2.46; N, 4.02%. Found: C, 22.63; H, 2.84; N, 4.42%. ^{1}H NMR (400 MHz, DMSO-d$_6$): *δ* 1.47 (t, *J* = 7.0 Hz, 6H, C*H*$_3$), 4.37 (t, *J* = 3.8 Hz, 4H, C*H*$_2$), 4.60 (q, *J* = 7.2 Hz, 4H, C*H*$_2$), 4.93 (s, 4H, C*H*$_2$), 7.29 (s, 2H, Ph*H*), 7.35 (m, 2H, Ph*H*), 7.75 (q, *J* = 6.4 Hz, 2H, Ph*H*), 7.90 (d, 2H, *J* = 6.0 Hz, Ph*H*), 7.91 (s, 2H, Ph*H*). ^{13}C NMR (100 MHz, DMSO-d$_6$): *δ* 175.7 (C_{carbene}), 146.9 (Ph*C*), 128.6 (Ph*C*), 126.3 (Ph*C*), 124.4 (Ph*C*), 123.8 (Ph*C*), 123.4 (Ph*C*), 107.0 (Ph*C*), 66.8 (O*C*H$_2$CH$_2$), 50.2 (OCH$_2$*C*H$_2$), 45.6 (*C*H$_2$CH$_3$), 16.4 (*C*H$_3$).

Preparation of [L^{2}Ag](PF$_6$) (7)

Silver oxide (0.092 g, 0.4 mmol) was added to a 1,2-dichloroethane/DMSO (15 mL, v:v = 2:1) solution of **L^{2}H$_2$·PF$_6$** (0.184 g, 0.2 mmol). The suspension was stirred for 24 h at 40 ˚C. The resulting solution was filtered and concentrated to 5 mL, and diethyl ether (5 mL) was added to precipitate a pale yellow powder. Isolation by filtration yielded complex **7**. Yield: 0.045 g (26%). M.p.: 252-254 ˚C. Anal. Calcd for $C_{40}H_{34}AgF_6N_6O_2P$: C, 54.37; H, 3.87; N, 9.51%. Found: C, 54.53; H, 3.62; N, 9.78%. ^1H NMR (400 MHz, DMSO-d$_6$): δ 4.39 (t, J = 4.2 Hz, 4H, CH_2), 5.05 (d, J = 4.0 Hz, 4H, CH_2), 5.92 (s, 4H, CH_2), 7.22 (s, 2H, ArH), 7.34 (m, 5H, ArH), 7.52 (m, 7H, ArH), 7.67 (q, J = 3.2 Hz, 2H, ArH), 7.77 (m, 2H, ArH), 7.97 (m, 2H, ArH), 8.50 (d, J = 4.4 Hz, 2H, ArH). ^{13}C NMR (100 MHz, DMSO-d$_6$): δ 155.5 (ArC), 149.5 (ArC), 147.3 (ArC), 137.2 (ArC), 133.8 (ArC), 132.8 (ArC), 128.5 (ArC), 126.1 (ArC), 124.17 (ArC), 124.10 (ArC), 123.2 (ArC), 122.2 (ArC), 112.4 (ArC), 111.8 (ArC), 106.7 (ArC), 65.6 (OCH$_2$CH$_2$), 53.2 (OCH$_2$$CH_2$), 48.3 (N$CH_2$).

Preparation of [L^{4}Ag](PF$_6$) (8)

This complex was prepared in a manner analogous to that for **8**, only **L^{4}H$_2$·PF$_6$** (0.170 g, 0.2 mmol) was used instead of **L^{2}H$_2$·(PF$_6$)$_2$**. Yield: 0.048 g (30%). M.p.: 248-250 ˚C. Anal. Calcd for $C_{36}H_{40}AgF_6N_4O_2P$: C, 53.14; H, 4.95; N, 6.88%. Found: C, 53.64; H, 4.78; N, 6.65%. ^1H NMR (400 MHz, DMSO-d$_6$): δ 0.92 (t, J = 11.4 Hz, 6H, CH_3), 1.44 (m, 4H, CH_2), 1.93 (m, 4H, CH_2), 4.40 (t, J = 4.2 Hz, 4H, CH_2), 4.64 (t, J = 6.8 Hz, 4H, CH_2), 5.14 (t, J = 4.0 Hz, 4H, CH_2), 7.23 (s, 2H, PhH), 7.30 (q, J = 3.2 Hz, 2H, PhH), 7.55 (m, 4H, PhH), 7.67 (q, J = 3.2 Hz, 2H, PhH), 7.90 (t, J = 4.4 Hz, 2H, PhH), 7.99 (t, J = 4.2 Hz, 2H, PhH). ^{13}C NMR (100 MHz, DMSO-d$_6$): δ 147.3 (PhC), 133.36 (PhC), 133.31 (PhC), 132.9 (PhC), 132.8 (PhC), 128.6 (PhC), 126.1 (PhC), 124.17 (PhC), 124.11 (PhC), 112.2 (PhC), 111.9 (PhC), 106.7 (PhC), 65.8 (OCH$_2$CH$_2$), 48.3 (OCH$_2$$CH_2$), 48.2($CH_2CH_2CH_2CH_3$), 31.9 (CH$_2$$CH_2CH_2CH_3$), 19.5 (CH$_2CH_2$$CH_2CH_3$), 13.5 (CH$_2CH_2CH_2$$CH_3$).

Fluorescence titrations

Fluorescence titrations were performed on a Cary Eclipse fluorescence spectrophotometer using a 1 cm path-length quartz fluorescence cell. The CH_3OH used in the titrations was freshly distilled. Titrations were carried out by placing the receptor **4** (1×10^{-5} mol/L) into the 4 mL cuvette and adding increasing amounts of the Ag^+ ($0\text{-}80.0 \times 10^{-5}$ mol/L) using a microsyringe. The solution of **4** was excited at 283 nm, and the emission spectra were recorded in the range of 316-394 nm. After each addition, an equilibration time of 8-10 min was allowed before the fluorescence intensity was recorded. Statistical analysis of the data was carried out using Origin 8.0.

UV titrations

UV titrations were performed on a JASCO-V570 spectrometer using a 1 cm path-length quartz cuvette. The CH_3OH used in the titrations was freshly distilled. Keeping the fixed overall concentration is 2.0×10^{-5} mol/L, and the molar fraction of Ag^+ was changed from 0 to 1. The absorption spectra were recorded in the range of 240-320 nm. After each addition, an equilibration time of 8-10 min was allowed before the absorption spectra were recorded. Statistical analysis of the data was carried out using Origin 8.

X-ray data collection and structure determinations

X-ray single-crystal diffraction data for complexes **1-8** were collected using a Bruker Apex II CCD diffractometer at 173(2) K for **1**, **3** and **7** and 296(2) K for **2**, **4-6** and **8** with Mo-Kα radiation (λ = 0.71073 Å) using the ω scan mode. There was no evidence of crystal decay during the data collection in all cases. Semiempirical absorption corrections were applied using SADABS and the program SAINT was used for the integration of the diffraction profiles.[27] All the structures were solved by direct methods using the SHELXS program of the SHELXTL package and refined with SHELXL[28] by the full matrix least-squares method, with anisotropic thermal parameters for all non-hydrogen atoms on F^2. Hydrogen atoms bonded to C atoms were placed geometrically and presumably solvent H atoms were first located in difference Fourier maps and then fixed in the calculated sites. Further details for the crystallographic data and structural analysis are listed in Tables S1-S3, generated using Crystal-Maker.[29]

Acknowledgments

This work was financially supported by the National Natural Science Foundation of China (No.21172172), Tianjin Natural Science Foundation (No.11JCZDJC22000) and The Program for Innovative Research Team in University of Tianjin (TD12-5038).

Supplementary Information

Text, tables, Figures and CIF files giving crystallographic data and the crystal packings for **1-8**, fluorescence and UV spectra for **4**, infrared **4** and **4**·$AgNO_3$, and general considerations, characterization data, and ^1H NMR and ^{13}C NMR spectra for all precursors and complexes with this article can be found in the online version.

References

1 (*a*) S. Lee, I. Choi, S. Hong, Y. I. Yang, J. Lee, T. Kang and J. Yi, *Chem. Commun.*, 2009, 6171-6173; (*b*) E. M. Nolan and S. L. Lippard, *Chem. Rev.*, 2008, **108**, 3443-3480.

2 (*a*) R. D. Hancock, *Chem. Soc. Rev.*, 2013, **42**, 1500-1524; (*b*) M. Formica, V. Fusi, L. Giorgi and M. Micheloni, *Coord. Chem. Rev.*, 2012, **256**, 170-192; (*c*) S. S. Huang, S. He, Y. Lu, F. F. Wei, X. S. Zeng and L. C. Zhao, *Chem. Commun.*, 2011, **47**, 2408-2410; (*d*) X. J. Peng, J. J. Du, J. L. Fan, J. Y. Wang, Y. K. Wu, J. Z. Zhao, S. G. Sun and T. Xu, *J. Am. Chem. Soc.*, 2007, **129**, 1500-1501; (*e*) H. N. Kim, M. H. Lee, H. J. Kim, J. S. Kim and J. Yoon, *Chem. Soc. Rev.*, 2008, **37**, 1465-1472; (*f*) M. H. Lee, S. W. Lee, S. H. Kim, C. Kang and J. S. Kim, *Org. Lett.*, 2009, **11**, 2101-2104.

3 (*a*) J. L. Barriada, A. D. Tappin, E. H. Evans and E. P. Achterberg, *TrAC-Trends Anal. Chem.*, 2007, **26**, 809-817; (*b*) H. T. Ratte, *Environ. Toxicol. Chem.*, 1999, **18**, 89-108.

4 C. M. Litwin, S. A. Boyko and S. B. Calderwood, *J. Bacteriol.*, 1992, **174**, 1897-1903.

5 (*a*) I. T. Ho, K. C. Haung and W. S. Chung, *Chem. Asian J.*, 2011, **6**, 2738-2746; (*b*) Z. Xu, S. Zheng, J. Yoon and D. R. Spring, *Analyst*, 2010, **135**, 2554-2559; (*c*) C. Zhao, K. Qu, Y. Song, C. Xu, J. Ren and X. Qu, *Chem. Asian J.*, 2010, **16**, 8147-8154; (*d*) H. H. Wang, L. Xue, Y. Y. Qian and H. Jiang, *Org. Lett.*, 2010, **12**, 292-295; (*e*) K. M. K. Swamy, H. N. Kim, J. H. Soh, Y. Kim, S. J. Kim and J. Yoon, *Chem. Commun.*, 2009, 1234-1236; (*f*) A. Chatterjee, M. Santra, N. Won, S. Kim, J. K. Kim, S. B. Kim and K. H. Ahn, *J. Am. Chem. Soc.*, 2009, **131**, 2040-2041; (*g*) R. Joseph, B. Ramanujam, A. Acharya and C. P. Rao, *J. Org.*

Chem., 2009, **74**, 8181-8190; (*h*) L. Liu, D. Zhang, G. Zhang, J. Xiang and D. Zhu, *Org. Lett.*, 2008, **10**, 2271-2274; (*i*) L. Liu, G. Zhang, J. Xiang, D. Zhang and D. Zhu, *Org. Lett.*, 2008, **10**, 4581-4584; (*j*) S. Iyoshi, M. Taki and Y. Yamamoto, *Inorg. Chem.*, 2008, **47**, 3946-3948; (*k*) X. Zhu, S. Fu, W. K. Wong and W. Y. Wong, *Tetrahedron Lett.*, 2008, **49**, 1843-1846; (*l*) J. Y. Lee, J. Kwon, C. S. Park, J. E. Lee, W. Sim, J. S. Kim, J. Seo, I. Yoon, J. H. Jung and S. S. Lee, *Org. Lett.*, 2007, **9**, 493-496; (*m*) A. Coskun and E. U. Akkaya, *J. Am. Chem. Soc.*, 2005, **127**, 10464-10465; (*n*) M. Hu, J. Fan, J. Cao, K. Song, H. Zhang, S. Sun and X. Peng, *Analyst*, 2012, **137**, 2107-2111.

6 D. Karunasagar, J. Arunachalam and S. Gangadharan, *J. Anal. At. Spectrom.*, 1998, **13**, 679-682.

7 Y. Li, C. Chen, B. Li, J. Sun, J. Wang, Y. Gao, Y. Zhao and Z. Chai, *J. Anal. At. Spectrom.*, 2006, **21**, 94-96.

8 (*a*) R. Rathore, V. J. Chebny and S. H. Abdelwahed, *J. Am. Chem. Soc.*, 2005, **127**, 8012-8023; (*b*) F. Wang, J. H. Moon, R. Nandhakumar, B. Kang, D. Kim, K. M. Kim, J. Y. Lee and J. Yoon, *Chem. Commun.*, 2013, **49**, 7228-7230; (*c*) T. Chen, W. Zhu, Y. Xu, S. Zhang, X. Zhang and X. Qian, *Dalton Trans.*, 2010, **39**, 1316-1320; (*d*) V. K. Bhardwaj, A. P. S. Pannu, N. Singh, M. S. Hundal and G. Hundal, *Tetrahedron*, 2008, **64**, 5384-5391; (*e*) K. M. K. Swamy, H. N. Kim, J. H. Soh, Y. Kim, S. J. Kim and J. Yoon, *Chem. Commun.*, 2009, 1234-1236; (*f*) B. Zhang, J. Sun, C. Bi, G. Yin, L. Pu, Y. Shi and L. Sheng, *New J. Chem.*, 2011, **35**, 849-853.

9 (*a*) O. Guerret, S. Sole, H. Gornitzka, M. L. Teichert, G. Teingnier and G. Berte, *J. Am. Chem. Soc.*, 1997, **119**, 6668-6669; (*b*) C. K. Lee, K. M. Lee and I. J. B. Lin, *Organometallics*, 2002, **21**, 10-12; (*c*) A. J. Arduengo III, H. V. R. Dias, J. C. Calabrese and F. Davidson, *Organometallics*, 1993, **12**, 3405-3409; (*d*) R. Z. Ku, J. C. Huang, J. Y. Cho, F. M. Kiang, K. R. Reddy, Y. C. Chen, K. J. Lee, J. H. Lee, G. H. Lee, S. M. Peng and S. T. Liu, *Organometallics*, 1999, **18**, 2145-2154.

10 (*a*) Q. X. Liu, Z. Q. Yao, X. J. Zhao, A. H. Chen, X. Q. Yang, S. W. Liu and X. G. Wang, *Organometallics*, 2011, **30**, 3732-3739; (*b*) Q. X. Liu, Z. Q. Yao, X. J.

Zhao, Z. X. Zhao and X. G. Wang, *Organometallics*, 2013, **32**, 3493-3501; (*c*) D. B. Qin, X. S. Zeng, Q. S. Li, F. B. Xu, H. B. Song and Z. Z. Zhang, *Chem. Commun.*, 2007, 147-149; (*d*) C. X. Lin, X. F. Kong, Q. S. Li, Z. Z. Zhang, Y. F. Yuan and F. B. Xu, *CrystEngComm*, 2013, **15**, 6948-6962.

11 (*a*) F. E. Hahn, M. C. Jahnke and T. Pape, *Organometallics*, 2007, **26**, 150-154; (*b*) P. L. Arnold and I. J. Casely, *Chem. Rev.*, 2009, **109**, 3599-3611; (*c*) F. E. Hahn and M. C. Jahnke, *Angew. Chem., Int. Ed.*, 2008, **47**, 3122-3172; (*d*) X. L. Liu and W. Z. Chen, *Organometallics*, 2013, **31**, 6614-6622; (*e*) Q. Li, X. Li, J. Yang, H. B. Song and L. F. Tang, *Polyhedron*, 2013, **59**, 29-37; (*f*) J. H. Chen, X. Q. Zhang, Q. Feng and M. M. Luo, *J. Organomet. Chem.*, 2006, **691**, 470-474; (*g*) J. Qu and Y. Cheng, *Tetrahedron*, 2013, **69**, 888-894; (*h*) B. Liu, Q. Xia and W. Z. Chen, *Angew. Chem., Int. Ed.*, 2009, **48**, 5513-5516.

12 (*a*) J. J. Van Veldhuizen, J. E. Campbell, R. E. Giudici and A. H. Hoveyda, *J. Am. Chem. Soc.*, 2005, **127**, 6877-6882; (*b*) J. C. Garrison and W. J. Youngs, *Chem. Rev.*, 2005, **105**, 3978-4008; (*c*) J. C. Y. Lin, R. T. W. Huang, C. S. Lee, A. Bhattacharyya, W. S. Hwang and I. J. B. Lin, *Chem. Rev.*, 2009, **109**, 3561-3598; (*d*) C. M. Crudden and D. P. Allen, *Coord. Chem. Rev.*, 2004, **248**, 2247-2273; (*e*) C. V. Georgios and H. G. Robert, *Chem. Rev.*, 2010, **110**, 1746-1787; (*f*) A. A. D. Tulloch, A. A. Danopoulos, S. Winston, S. Kleinhenz and G. Eastham, *Dalton Trans.*, 2000, 4499-4506; (*g*) X. Wang, S. Liu, L. H. Weng and G. X. Jin, *Organometallics*, 2006, **25**, 3565-3569; (*h*) L. H. Gade and S. Bellemin-Laponnaz, *Coord. Chem. Rev.*, 2007, **251**, 718-725; (*i*) B. Liu, C. Y. Chen, Y. J. Zhang, X. L. Liu and W. Z. Chen, *Organometallics*, 2013, **32**, 5451-5460; (*j*) X. Q. Zhang, Y. P. Qiu, B. Rao and M. M. Luo, *J. Organomet. Chem.*, 2009, **28**, 3093-3099; (*k*) J. W. Wang, Q. S. Li, F. B. Xu, H. B. Song and Z. Z. Zhang, *Eur. J. Org. Chem.*, 2006, 1310-1316; (*l*) Q. Li, Y. F. Xie, B. C. Sun, J. Yang, H. B. Song and L. F. Tang, *Organometallics*, 2013, **745**, 106-114.

13 A. L. Pickering, G. Seeber, D. L. Long and L. Cronin, *CrystEngComm*, 2005, **7**, 504-510.

14 (*a*) S. Ahrens, A. Zeller, M. Taige and T. Strassner, *Organometallics*, 2006, **25**, 5409-5415; (*b*) W. A. Herrmann, *Angew. Chem., Int. Ed.*, 2002, **41**, 1290-1309; (*c*) J. P. Knowles and A. Whiting, *Org. Biomol. Chem.*, 2007, **5**, 31-44.

15 Q. X. Liu, J. Yu, X. J. Zhao, S. W. Liu, Z. Q. Wang, A. H. Chen and X. G. Wang, *CrystEngComm*, 2011, **13**, 4086-4096.

16 (*a*) D. J. Nielsen, K. J. Cavell, B. W. Skelton and A. H. White, *Organometallics*, 2006, **25**, 4850-4856; (*b*) J. Huang, E. D. Stevens and S. P. Nolan, *Organometallics*, 2000, **19**, 1194-1197; (*c*) Q. X. Liu, S. J. Li, X. J. Zhao, Y. Zang, H. B. Song, J. H. Guo and X. G. Wang, *Eur. J. Inorg. Chem.*, 2010, **2010**, 983-988.

17 (*a*) Q. X. Liu, L. N. Yin and J. C. Feng, *J. Organomet. Chem.*, 2007, **692**, 3655-3663; (*b*) U. J. Scheele, S. Dechert and F. Meyer, *Inorg. Chim. Acta*, 2006, **359**, 4891-4900; (*c*) K. M. Lee, J. C. C. Chen, C. J. Huang and I. J. B. Lin, *CrystEngComm*, 2007, **9**, 278-281.

18 M. L. Cole and P. C. Junk, *CrystEngComm*, 2004, **6**, 173-176.

19 (*a*) Q. X. Liu, X. J. Zhao, X. M. Wu, L. N. Yin, J. H. Guo, X. G. Wang and J. C. Feng, *Inorg. Chim. Acta*, 2008, **361**, 2616-2622; (*b*) R. P. A. Bettens, D. Dakternieks, A. Duthie, F. S. Kuan and E. R. T. Tiekink, *CrystEngComm*, 2009, **11**, 1362-1372.

20 (*a*) H. J. Kim, S. H. Kim, H. Kim, L. N. Anh, J. H. Lee, C. H. Lee and J. S. Kim, *Tetrahedron Lett.*, 2009, **50**, 2782-2786; (*b*) J. F. Zhang, Y. Zhou, J. Yoon, Y. Kim, S. J. Kim and J. S. Kim, *Org. Lett.*, 2010, **12**, 3852-3855; (*c*) L. Xue, C. Liu and H. Jiang, *Org. Lett.*, 2009, **11**, 1655-1658.

21 (*a*) J. Polster and H. Lachmann, *Spectrometric Titrations*, VCH, Weinheim, 1989, 256-259; (*b*) J. Wang, S. G. Bodige, W. H. Watson and C. D. Gutsche, *J. Org. Chem.*, 2000, **65**, 8260-8263.

22 G. Shyamaprosad, H. Anita, C. Rinku and K. F. Hoong, *Org. Lett.*, 2009, **11**, 4350-4353.

23 A. Easwaran, A. Ayyappanpillai and D. Jorg, *J. Am. Chem. Soc.*, 2005, **127**, 3156-3164.

24 (*a*) J. Dessingou, A. Mitra, K. Tabbasum, G. S. Baghel and C. P. Rao, *J. Org. Chem.*, 2012, **77**, 371-378; (*b*) K. Velmurugan, A. Raman, S. Easwaramoorthi and R. Nandhakumar, *RSC Adv.*, 2014, **4**, 35284-35289; (*c*) G. N. Lin, H. Xu, Y. J. Cui, Z. Y. Wang, Y. Yang and G. D. Qian, *Mater. Chem. Phys.*, 2013, **141**, 591-595; (*d*) C. Y. Li, X. F. Kong, Y. F. Li, C. X. Zou, D. Liu and W. G. Zhu, *Dyes Pigments*, 2013, **99**, 903-907; (*e*) H. Zheng, M. Yan, X. X. Fan, D. Sun, S. Y. Yang, L. J. Yang, J. D. Li and Y. B. Jiang, *Chem. Commun.*, 2012, **48**, 2243-2245.

25 (*a*) H. Ruffin, S. A. Baudron, D. Salazar-Mendoza and M. W. Hosseini, *Chem. Eur. J.*, 2014, **20**, 2449-2453; (*b*) S. V. Lindeman, R. Rathore and J. K. Kochi, *Inorg. Chem.*, 2000, **39**, 5707-5716.

26 Y. Habata, A. Taniguchi, M. Ikeda, T. Hiraoka, N. Matsuyama, S. Otsuka and S. Kuwahara, *Inorg. Chem.*, 2013, **52**, 2542-2549.

27 Bruker AXS, *SAINT Software Reference Manual*, Madison, WI, **1998**.

28 Sheldrick, G. M. *SHELXTL NT (Version 5.1), Program for Solution and Refinement of Crystal Structures*, University of Göttingen, Göttingen(Germany), **1997**.

29 Palmer, D. C. *Crystal Maker 7.1.5, CrystalMaker Software*, Yarnton, UK, **2006**.

A table of contents entry:

Seven NHC macrometallocycles (Hg(II) and Ag(I)) were prepared, and the recognition of Ag^+ using $(NHC)_2$-Hg-I_2 (**4**) as a host was studied.

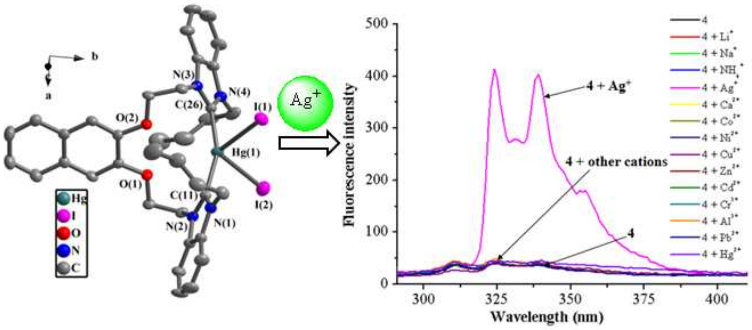

Software of graphics:

Schemes 1-3: Chem Draw 8.0

Figures 1-8: Diamond 3.0

Figures 9-11: Origin 8.0